THE REATTACHMENT OF LAMINAR CAVITY FLOW WITH HEAT TRANSFER AT HYPERSONIC SPEED

by

Paul K. Chang

Technical Report

AFOSR 66-0135

Submitted to

U. S. Air Force
Office of Scientific Research
Washington, D. C.

April 30, 1966

The Catholic University of America
Department of Mechanical Engineering
Washington, D.C. 20017

The Reattachment of Laminar Cavity Flow with Heat Transfer at Hypersonic Speed

by

Paul K. Chang

Technical Report

AFOSR 66-0135

Submitted to

United States Air Force
Office of Scientific Research
Washington, D. C.

April 30, 1966

The Catholic University of America
Department of Mechanical Engineering
Washington, D. C. 20017

Foreword

This analytical investigation has been carried out in Spain and Germany during the period of the sabbatical leave 1965-1966.

The research was supported in its entirety by the United States Air Force, Office of Scientific Research, Contract AF-AFOSR-706-6[illegible]

The author wishes to thank the United States Air Force, Office of Scientific Research for its generous support.

The Reattachment of Laminar Cavity Flow with Heat Transfer At Hypersonic Speed

Summary

A study of cavity flow is made based upon the analysis of a physical model and by referring to the experimental data of a particular test model with the reattachment surface perpendicular to free stream direction at free stream Mach number of eleven.

The pressure and heat transfer in the reattachment zone may be predicted approximately by the flow quantities along the dividing stream line employing the mixing theory and stagnation heat transfer equation for a blunt body. Good agreement with experimental data is obtained.

It is found that the value of the average mixing rate correlation function for the cavity flow is 15 and is equal to that value determined by Glick for separated flow caused by shock impingement. Semi-empirically, efficiency factor of compression equal to 0.67 at the reattachment is evaluated and the reattachment velocity gradient parameter for the particular test model is similar to this case of stagnation flow over blunt nose. It appears that the heat transfer at the reattachment surface perpendicular to the free stream direction may be predicted approximately by the stagnation point heat transfer equation for a two-dimensional blunt surface.

Table of Contents

List of Figures

Nomenclature

A	constant, $A = 0.44$
a	velocity of sound
a_1	constant
$C(\kappa)$	mixing rate correlation function
$\overline{C}$	average value of C
C, C_1, C_2	constants
c_f	skin friction coefficient
c_p	specific heat at constant pressure
D	depth of cavity
d	diameter, $d = 2D$
F	$F = \frac{f}{\kappa^2} - 1$
f	T_1/T_t
f_2	factor
g	gravity
H	stagnation enthalpy
h	heat transfer coefficient $h = \frac{q}{T_w - T_{aw}}$
I	mass flux in x-direction, $I = \int_0^{\delta} u^2 \, dy$
k	$k = \frac{d\delta}{dx} - \theta$
L	length of cavity
L_R	reattachment zone length
ℓ	distance from forward stagnation point to the separation point
M	Mach number

$\bar{m}$	mass flux in x-direction, $\bar{m} = \int_0^{\delta} \rho\, u\, dy$
p	static pressure
Pr	Prandtl number
R	Rankine
$\mathcal{R}$	gas constant
Re	Reynolds number
r_o	radius of cross-section of body of revolution
$\bar{s}$	coordinate along the reattachment surface
St	Stanton number
T	temperature
u	velocity component in x-direction
u^*	$u^* = u_d/u_e$
$u_{\bar{s}}$	velocity component in $\bar{s}$-direction
w	$w = u/a_t$
x, y	coordinates along and normal to the dividing stream line
α	constant in linear relation of $F = \alpha \kappa + \bar{\beta}$
β	angle between dividing stream line and reattachment wall
$\bar{\beta}$	constant in linear relation of $F = \alpha \kappa + \bar{\beta}$
Γ_o, Γ_1	vortices inside and outside the stagnating stream line
γ	ratio of specific heats, $\gamma = c_p/c_v$
δ	physical thickness of viscous layer
δ^*	displacement thickness of viscous layer
δ^{**}	momentum thickness of viscous layer
η	$\eta = F_o/F$

θ	stream line direction relative to wall at y = δ
κ	Crocco-Lees velocity profile shape parameter
λ	parameter
μ	dynamic viscosity
ν	kinematic viscosity
ξ	efficiency factor of compression relative to that of an isentropic process
ρ	density
τ	shear stress
φ_e	$\varphi_e = \frac{1 - \frac{\gamma - 1}{2} w_e^2}{\gamma \cdot w_e}$
φ_1	$\varphi_1 = (T_1/T_t) / (\gamma w_1)$
ψ	stream function
Ω	$\Omega = F/\kappa$
ω	$\omega = \kappa_o/\kappa$

Superscript

'	condition downstream of reattachment

Subscripts

av	average
aw	adiabatic wall
c	cone
cav	cavity
d	dividing stream line
e	conditions at y = δ in the cavity zone
i	incompressible

o	beginning of reattachment zone
ℓ	reattachment
S	separation
$\bar{s}$	along $\bar{s}$ direction
t	total temperature
w	wall
1	mean value of viscous region
∞	free stream

Introduction

The problem of cavity flow which involves separation as well as reattachment is complicated and, as yet, not completely understood. The solution of this problem is not only for the interest of basic science but also important fo many practical applications. For example, for a cut-out in a structure surfa such as a bomb bay, open cock pit, escape hatch, etc.; the heat transfer at th reattachment zone may become very high at the hypersonic flight speeds.

The pronounced features of cavity flow are viscous momentum transfer along the boundary stream line of the cavity opening and the circulating flow within the cavity. The momentum is transferred from the external flow to the internal flow due to viscous mixing and the flow within the cavity circulating t balance the mass rate flow.

For subsonic flow the concept of mass balance between the outgoing and incoming fluid from and into the idealized wake model has been used by Tanne to predict with a simple analysis the drag and base pressure of cones as well the area of outgoing flow from the wake. However, no consideration is given the viscous momentum transfer.

For supersonic laminar separated and reattached flow Chapman [2, 3] Crocco-Lees [4] developed the detailed mixing theory for the interaction betw viscous internal flow and the nearly isentropic external stream. Chapman [2 troduced the idea of the so-called "dividing stream line" which divides the flow field within the very deep cavity into two zones, i.e., outside by pass flow zon of this stream line and inside zone of circulating flow, and obtained an exact similarity solution for the velocity profile of the mixing layer. A simplified

calculation showed that the reattachment process is essentially isentropic.

The Crocco-Lees' theory is general and applicable qualitatively for a wide range of separated flow problems. The separated and reattached flows are characterized by two governing parameters of κ and f defined by boundary layer thickness. Much of the complex phenomena of the separated and reattached flow are clarified by this theory. Glick [5] used Chapman's flow model which incorporates the concept of the "dividing stream line" to apply the Crocco-Lees' theory. This model has been translated into Crocco-Lees language by the semi-empirical approach. Glick found that the cause of poor quantitative prediction of Crocco-Lees' theory was an incorrect mixing rate correlation function C (κ), thus by determining the proper approximate C (κ) - F (κ) relation where $F = \frac{f}{\kappa}2 - 1$ for separated and reattached flow a good agreement with experimental data was obtained for the pressure distribution in the region of separated flow caused by shock interaction.

Restricting to a moderately compressible separated flow over the concave surface, Bloom [6] obtained solutions for velocity gradient, pressure, boundary layer thickness employing an integral method and emphasizing the reverse flow profiles.

For the supersonic turbulent reattachment flow behind a step, Chapman-Korst [7, 8] established a recompression criterion of reattachment and McDonald [9] improved this criterion. McDonald formulated a transformed shape parameter for the boundary layer by using Stewartson-Illingworth transformation to specify the reattachment.

For the solution of slow circulating flow within the cavity, Squire [10] proposed an analytical approach to divide the cavity zone into two parts; the

inside part of "core" and the outside part of the boundary layer which surrounds the core. The motion in the cavity is maintained by the shear stress of the outer flow acting on the stream line boundary of the cavity. Mills [11] obtained analytically the velocity profiles along the square cavity wall based upon Squire idea and his results are in a good agreement with the experimental data.

Batchelor [12] proposed a model of a finite laminar separated flow region for a two-dimensional as well as axial symmetric cavity with limiting steady flow at high Reynolds number. In this model an inviscid rotational core is separated from the external flow by a recirculating viscous shear layer. Since this cavity model does not provide the unique flow field, the recirculating flow is divided further into a cellular substructure of eddies each satisfying the Batchelor's conditions.

Burggraf [13] applied this Batchelor's model to analyze the flow and heat transfer in rectangular cavities of various depths by employing an approximate linear theory in order to account for the effect of cavity depth by a correlation factor. For convenience, the problem is broken up into several parts and each is analyzed separately, then by matching these partial solutions the complete solution is synthesized. Burggraf's [13] incompressible flow analysis can be extended to compressible flow, but his analysis predicts a pressure lower than that obtained by experiment at the reattachment.

Most recently Burggraf [14] carried out an extensive analysis of incompressible flow for the viscous structure of a separated eddy within a fixed finite cavity as a function of the Reynolds number. In particular he considered the square cavity and determined the velocity profile, distributions of skin friction and total power. The thermal condition in a recirculating eddy is considered,

but no specific information is available for the pressure and heat transfer at the reattachment.

On the heat transfer of the laminar cavity flow Chapman [3] succeeded only to compute the average heat transfer rate amounting to 0.56 of that of the attached flow. For the determination of the local heat transfer rate the flow solution which considers the effects of the circulating flow and the relation of flow direction with respect to surface configuration should be known. Chung and Viegas [15] determined analytically the velocity distribution along the reattachment wall of the cavity, assuming that the reattachment flow is laminar, two-dimensional as well as incompressible but rotational. They further assumed that the reattachment of the flow along the dividing stream line takes place normal to the reattachment surface. By using their analytical results and a semi-empirical formula for heat transfer, an average value of the heat transfer in the reattachment zone was obtained. Burggraf's [13] analytical solution at the reattachment results in the square root singularity.

Carlson [16] determined the local heat transfer for laminar separated flow upstream of reattachment behind a step of a body of revolution at hypersonic speed taking into account a velocity profile of reverse flow. It has been assumed that no chemical reaction and no mass addition of fluid takes place, the cavity pressure is constant throughout the region, and the dividing stream line is straight. Although it was shown that the rate of heat transfer increases approaching reattachment, no detailed information on the reattachment heat transfer is available. Recently Korst [17] developed the generalized analysis of dynamics and thermodynamics of separated flow.

This review of references shows that up to date no reliable analysis for the laminar local properties of reattachment flow and the heat transfer for the cavity has been developed. Therefore, for the first step of the investigation based on two flow models of Chapman and Squire an attempt is made to find out whether the existing analysis can be applied for reattachment of the cavity flow.

Various experiments on the flow and heat transfer of cavity have been carried out in the past. In the region of subsonic speeds, Roshko [18] measure pressure and velocity distributions on the wall of rectangular cavity by varying the ratios of depth to length of cavity. Tani [19]measured longitudinal compon of mean velocity, turbulent intensity and turbulent shear stress across several traverse sections of rectangular cavity. Maull and East [20] discovered exper mentally over the bottom of rectangular cavities, the three-dimensional cellula flow pattern between certain range of ratio of cavity length to width, but Fox [2 did not notice it. However, Fox [21] indicates that there exists the distinct flo regime in the pressure coefficient and velocity profile and used them to identify the range of ratio of length to width of cavity with different flow regime.

In the range of supersonic speeds, by using rectangular cavities, Charw [22] evaluated the pressure distribution on the floor and recompression surface as well as velocity distribution through shear layer. Furthermore, the variatic of heat transfer distribution on the floor was measured. Larson [23] determin for laminar and turbulent flow the average heat transfer for the cavity formed on an axially symmetric body at free stream Mach numbers up to 4 and also the streamwise distribution of heat transfer including the reattachment zone. Bogdonoff and Vas [24] measured distributions of pressure and heat transfer over the cone-cavity model at $M_\infty \approx 11.7$. More recently, Nicoll [25] carried

out extensive measurements on streamwise pressure and heat transfer distributions for cut-outs on cones using helium as a fluid medium at free Mach numbers of 11 and 20. These results show that Chung-Viegas' results of average reattachment heat transfer are about twice those obtained in these experiments. The existing experimental data are useful to evaluate semi-empirically reattachment flow parameters such as reattachment velocity gradient and efficiency factor of compression and confirm the applicability of the existing analysis to cavity flow.

1. Physical Model of Cavity Flow

For the investigation of flow in the region of the cavity, a physical model as shown in Figure 1 is proposed. This model divides the whole flow field into two regions by the dividing stream line, i.e., the external nearly isentropic flow region and the internal viscous flow region. This represents basically the Chapman's model [2] as sketched in Figure 1 except for the shaded area within the cavity. This model emphasizes the viscous mixing process of the external flow with the internal flow.

The velocity profile at the separation point S is similar to that at the reattachment point R where shear stress is zero. The fluid particle which is adjacent to the wall at the separation must be adjacent to the wall at the reattachm and the external flow may be considered as an essentially by-pass flow. Due t the viscosity of the fluid, mixing of external fluid with internal fluid takes plac in the mixing layer which extends from the separation point to the beginning of reattachment zone. But with the presence of heat transfer, at supersonic spe the process of mass exchange may be considered as quasi-steady, and the cor responding values at the proper flow properties are taken for the analysis, si the dividing stream line may fluctuate and periodic mass transfer can take pla as evidenced by Charwat [22] for the rectangular cavity. The thickness of the thin mixing layer grows parabolically with downstream distance from the orig of mixing but the rate of growth is about three times larger than that of the attached laminar layer.

The internal flow field is a circulating flow region and this flow field may be divided again into two regions, i.e., the inner "core" and the outer thin boundary layer belt surrounding the core as proposed by Squire [10] for subs

speed. Figure 2 illustrates the recirculating cavity flow while the shaded area of Figure 1 indicates the core. Within the core the mass entrained from the so-called dead air region where the velocity is small but not necessarily zero, (i.e., the region below the zero velocity line) and the mass reversed back into the dead air region to balance each other and are responsible for the maintenance of the circulatory flow within the cavity. The back flow is caused by the pressure rise in the reattachment zone [Figure 3] and the mass balance causes the pressure of cavity to differ from that upstream of separation.

Recent analytical investigation of Denison and Baum [26] by solving numerically the governing differential equations on a computer showed that sufficiently downstream of the separated flow region $u^* = u_d/u_e$, defined as the ratio of laminar flow velocity along the dividing stream line and the potential stream line outside the cavity, is $u^* = 0.587$ regardless of whether it is axi-symmetric or two-dimensional flow. This result is obtained by considering an initial boundary layer thickness at the separation. On the other hand for two-dimensional laminar flow, Chapman [2, 7] obtained analytically the same value of u^* under the assumption of zero boundary layer thickness at the separation. Hence, it may be concluded that if the reattachment distance is small compared to the whole cavity length, the reattachment process can be investigated separately apart from the upstream conditions where the momentum transfer up to the initial pressure rise for reattachment is known.

In the reattachment zone the pressure rises as shown in Figure 3 because ot the increased momentum in the shear layer due to viscous mixing, and the deceleration of the flow. Since at the reattachment the velocity is zero, a particle moving along the stream line within the mixing layer must be able to

overcome the pressure rise and therefore in order to pass through the downstream direction, its total pressure at the reattachment must be larger than p', the static pressure downstream of the reattachment. Thus although particl (a) (see Figure 3) may pass through reattachment, particle (b) may not, becau its velocity is lower than that corresponding to the pressure at the reattachmer equal to p'. Therefore, particle (b) is reversed back. Chapman et al [7] observed that the reattachment pressure rise is independent of Reynolds number. Furthermore, as indicated in Figure 4, Harper [27] found that if the incompressible flow stagnates on a flat surface then the flow region in the neighborhood of the stagnation point is inviscid, although the stagnation point itself lies in the viscous layer. Hence, the reattachment process approaching the reattachment point may be considered as isentropic but in the very close regio near the reattachment as well as at the reattachment point itself viscosity effec should be included. Besides the effect of compressibility, geometrical relatio for the reattaching stream line to the reattaching wall, etc. are also to be considered to evaluate the flow properties at the reattachment correctly.

Similar to the stagnating flow process, the flow velocity reduces to zero a the reattachment point but its velocity gradient is finite. The flow velocity alo the reattaching surface may be computed based upon the cavity flow model in the core and surrounding boundary layer. Since heat transfer in the stagnation region, can be evaluated by knowing the velocity gradient at the stagnation poin and the velocity distribution around it, the heat transfer, in the reattachment zone may also be solved based upon the flow model proposed here.

2. Pressure Rise in the Reattachment Zone

The pressure rise in the reattachment zone of the cavity is determined analytically and its numerical values are evaluated semi-empirically.

The reattachment pressure rise is due to momentum transfer upstream of reattachment and deceleration in the reattachment zone. The mass transfer is computed by the method of Glick [5] and the deceleration of flow by Harper's [27] formula.

The coordinate system is indicated in Figure 5. The origin of the coordinate is located at the separation point with the x-axis along the dividing stream line and the y axis perpendicular to x-axis. If the coordinate along the zero velocity line [Figure 1] is designated by $\bar{x}$, which corresponds to imaginary wall-coordinate then the direction of x is approximately equal to that of $\bar{x}$ downstream of the separation point in the mixing zone. The initial point of the pressure rise for the reattachment is denoted by subscript o.

For the analysis the following assumptions are made:

1. Cavity is open, i.e., the dividing streamline bridges the cavity from separation to reattachment and does not attach on the cavity floor. L/D is sufficiently small so that the streamwise pressure gradient from separation to the initial point of the pressure rise is zero. The location of the initial point for reattachment pressure rise is considered known.
2. Pressure gradient traverse to the stream direction is zero.
3. Flow is quasi-steady and gas is thermally as well as calorically perfect. The property values of flow are interpreted properly as such.
4. The gradient of viscious or Reynolds stress in the flow direction are negligible compared to the static pressure gradient in the flow direction.

5. Theory of Crocco-Lees for two-dimensional flow is applicable for axially symmetric flow.

6. Heat transfer effect is negligible for the computation of pressure rise

7. The pressure rise prior to the initial point of reattachment is negligil

For a streamline within the mixing layer with angle, $\frac{d\delta}{dx} - \theta$, between streamline and the outer boundary of the dissipative flow, at $y = \delta$, [Figure the governing equations are;

$$\frac{d\bar{m}}{dx} = \rho_e u_e \left[\frac{d\delta}{dx} - \theta \right] = k \rho_e u_e \qquad (1)$$

where $k = \frac{d\delta}{dx} - \theta$ is mixing coefficient and θ is streamline direction an relative to the wall at $y = \delta$.

This equation expresses the rate at which mass is transferred from exte flow to internal flow due to mixing and

$$\frac{dI}{dx} = u_e \left(\frac{d\bar{m}}{dx} \right) - \delta \frac{dp}{dx} - \tau_w \qquad (2)$$

where $I = \int_0^{\delta} \rho u^2 \, dy$ -- momentum flux in x-direction

$\bar{m} = \int_0^{\delta} \rho u \, dy$ -- mass flux in x-direction

is the momentum equation in x-direction.

These definitions are referred to the limit o and δ, i.e., the partially truncated thickness of the viscous layer measured from the axis to the dividir steamline of the outer edge of the viscous layer as shown in Sketch A

By referring to the total thickness of the viscous layer δ_t, as shown in Sketch B, it may be postulated that the mass flow rates for both (profiles as shown in Sketch A and Sketch B) remain the same, although $\delta < \delta_t$.

Consider two different portions of the flow path. The first consists of a constant mass rate of circulatory flow along b path below the zero velocity lir

(Sketch C), say m_c and another consist of the mass rate of the by-pass flow over the zero velocity line, say m_p which corresponds to that indicated by Sketch B.

Now consider the divided flow fields above and below the dividing streamline. Then due to the viscous mixing effect between the dividing stream line and zero velocity line and the breathing of cavity, an additional mass $\Delta\bar{m}$ is entrained and this $\Delta\bar{m}$ flows out from the cavity, along path a (Sketch C) in order to maintain m_c inside the cavity. Hence, $\Delta\bar{m}$ is ejected from the cavity into the viscous mixing layer as observed by Charwat et al [22] for the supersonic cavity flow. Tani [28] observed also the mass ejection from the separated flow region behind a step across the dividing stream line at subsonic free stream velocity. Hence at the same distance from the top of profile of Sketch A and B in negative y direction it may be assumed that $\rho . u > \rho' . u'$ and the mass flow rate over the dividing stream line in the region of shortened viscous layer $\int_o^{\delta} \rho\, u\, dy$ as shown in Sketch A is postulated to be equal to $\int_o^{\delta_t} \rho' u' dy$ which is based on a hypothetical profile with no entrainment from the inner cavity where δ_t is its actual thickness of the viscous layer.

The definition of momentum flux in x-direction I is made by an integration from dividing stream line to δ, similar to the mass flux in x-direction $\bar{m}$.

For the external isentropic flow, the Bernoulli's equation is,

$$\frac{1}{p}\frac{dp}{dx} = -\frac{1}{\psi_e}\frac{dw_e}{dx} \qquad (3)$$

where $\psi_e = \left\{ 1 - \left(\frac{\gamma - 1}{2} w_e^2\right) \right\} / \gamma w_e$

$\gamma = c_p / c_v$

$w_e = u_e / a_t$

and $a_t = \sqrt{\gamma \mathcal{R} T_t}$ -- stagnation speed of sound.

In order to compute the momentum transfer in a region between separat: and the beginning of reattachment and pressure rise in the reattachment zone these equations are cast into the language of Crocco-Lees [4] using Glick's [improved method.

A basic non-dimensional shape parameter is defined by

$$\kappa = \frac{I}{\bar{m}\, u_e} = \frac{\text{momentum flux}}{\text{mass flux times local external velocity}}$$

$$\text{or } \kappa = \frac{u_1}{u_e} = \frac{\text{actual momentum flux}}{\text{momentum flux of mass flux moving at } u = u_e}$$

where subscript 1 refers to average value of viscous region.

This parameter κ has the ability to correlate the velocity profile in the pr sure plateau region of the separated flow which is different from the known Bl flow.

The two key correlations of $F(\kappa)$ and $C(\kappa)$ for the solution of the separat and reattached flow are formulated by κ as follows:

$$F(\kappa) = \frac{f}{\kappa^2} - 1 \qquad \text{where} \quad f = \frac{T_1}{T_t} + \frac{\gamma - 1}{2} \kappa^2 w_e^2$$

$$\text{and} \quad C(\kappa) = \frac{k\,\bar{m}}{\mu_e} = \frac{(d\bar{m}/dx) / (\rho_e u_e)}{\mu_e / \bar{m}}$$

T, ρ, μ are temperature, density and dynamic viscosity respectively and the subscript t refers to total temperature.

Then the continuity, momentum and Bernoulli's equations are reduced to

$$\frac{dm}{dx} = \frac{p}{\rho_e} k \tag{4}$$

$$\frac{d}{dx}(m\, k\, w_e) = w_e \frac{dm}{dx} - \rho \frac{dp}{dx} - \frac{p w_e}{\rho_e} \frac{c_f}{2} \tag{5}$$

$$\text{and} \quad \frac{dp}{p} = - \frac{d w_e}{\rho_e} \tag{6}$$

where $m = \bar{m} \cdot a_t$.

Since upstream of reattachment, $\frac{dp}{dx}$ and c_f are negligible, momentum equation (5) reduces to

$$\frac{d}{dx} \quad (m \; k \quad w_e) = \quad w_e \quad \frac{dm}{dx} \tag{7}$$

of $$\frac{1}{1 - \kappa} \quad \frac{d\kappa}{dx} \quad = \quad \frac{1}{m} \quad \frac{dm}{dx}$$

By integrating from separation point to the initial point of reattachment zone,

$$\kappa_o = 1 - (1 - \kappa_s) \; \frac{m_s}{m_o}$$

where the subscript s and o refer to separation and initial point of reattachment respectively. From this equation it is seen that the levels of momentum and energy in the viscous region are raised by mass entrainment, because for $m_o > m_s$, $\kappa_o > 1$.

Since

$$\frac{dm}{dx} = \frac{p}{\varphi_e} \; k = \frac{C(\kappa)}{m} \quad \frac{p}{\varphi_e} \; \mu_e \, a_t$$

and

$$\frac{p}{\varphi_e} = \frac{p}{\frac{T_e}{T_t} \; \frac{1}{\gamma \; w_e}} = p \; \gamma \; \frac{T_t}{T_e} \; \frac{u_e}{a_t} = \; e u_e a_t$$

it follows

$$\frac{dm}{dx} \quad = \quad \frac{C(\kappa)}{m} \quad \rho_e \, u_e \, \mu_e \, a_t^{\,2} \tag{8}$$

The increase of mass flow due to entrainment can be evaluated by integrating this equation, if the relation of $C(\kappa)$ with respect to x is known. Although it is expected that $C(\kappa)$ starts at zero and rises near separation, for simplicity an average constant value of $\bar{C}$ is used and its numerical value is determined properly from experimental data.

Then by integrating equation (8),

$$m_o^{\,2} - m_s^{\,2} \quad = \quad 2 \, \bar{C} \quad \rho_e \, u_e \, \mu_e \, a_t^{\,2} \quad x_o$$

$$\text{or} \qquad \frac{m_o}{m_s} = \sqrt{1 + \frac{2\, Re_{xo}\, \bar{C}\, a_t^2\, \mu_e^2}{m_s^2}} \qquad (9)$$

Where x_o is streamwise distance from separation to the beginning of reattachment and $Re_{xo} = \dfrac{\rho_e u_e x_o}{\mu_e}$

Taking $$\frac{\bar{m}_s \cdot a_t}{\mu_t} = \frac{T_e}{T_t} \frac{Re_{\delta}^{**}}{1 - \kappa} \qquad \text{(Ref. 30)}$$

and $$Re_{\delta}^{**} = \sqrt{A}\ \sqrt{Re_x} \qquad \text{(Ref. 5)}$$

$$\kappa_o = 1 - \frac{1 - \kappa_s}{\sqrt{1 + \dfrac{2(1-\kappa_s)^2\, \bar{C}}{A} \cdot \dfrac{x_o}{\ell}}}$$

The value of A may be taken $A = 0.44$ and ℓ is the distance from the stagnation point to the separation point.

Since in the reattachment zone the streamwise pressure rise may be computed by flow quantities along the dividing stream line [7], and mixing rate and viscous term are negligible, the momentum equation (5) is reduced to

$$\frac{d}{dx}\left(m \kappa w_d\right) = -\delta \frac{dp}{dx} \qquad (10)$$

where the subscript d refers to dividing stream line

Since $m = \rho \delta / \varphi_1$,

it follows $$d\kappa + \kappa \frac{dw_d}{w_d} = -\frac{\varphi_1}{w_d} \frac{dp}{p}$$

but $$\varphi_1 = \frac{\kappa}{\gamma w_d}\left(F + \frac{T_d}{T_t}\right)$$

thus $$d\kappa = -\kappa \frac{dw_d}{w_d} + \kappa \left[F \frac{T_t}{T_d} + 1\right] \frac{dw_d}{w_d}$$

Because $$\frac{dw_d}{w_d}\left(\frac{T_t}{T_d}\right) = \frac{dM_d}{M_d}$$

finally $$d\kappa = \kappa F \frac{dM_d}{M_d} \qquad (11)$$

In order to integrate this equation, a relation of F with respect to κ must be known.

In the reattachment zone, a linear relation of F with respect to κ may be assumed [5],

thus

$$F = \alpha \kappa + \bar{\beta} \qquad (12)$$

where α and $\bar{\beta}$ are constants depending on the values of F_o and κ_o.

Hence equation (11) becomes

$$\frac{d\kappa}{\alpha \kappa^2 + \bar{\beta}} = \frac{d M_d}{M_d}$$

Integrating from the beginning point of reattachment to downstream distance.

$$M_{do} = M_d \left[\frac{\kappa_o}{\kappa} \left(\frac{\kappa + \bar{\beta}/\alpha}{\kappa_o + \bar{\beta}/\alpha} \right) \right]^{\frac{1}{\bar{\beta}}} \qquad (13)$$

Putting

$$\Omega = F / \kappa$$

$$\eta = F_o / F$$

$$\omega = \kappa_o / \kappa$$

it follows;

$$\alpha = \Omega (\eta - 1) / (\omega - 1)$$

$$\bar{\beta} = F (\omega - \eta) / (\omega - 1)$$

and equation (13) is rewritten by

$$M_{do} = M_d \left(\frac{\omega}{\eta} \right)^{\frac{-(\omega - 1)}{F(\eta - \omega)}} \qquad (14)$$

The value of F_o is taken as $F_o = F_s = 2.85$ [5].

Assuming the isentropic compression, the pressure rise in the reattachment zone is given by

$$\frac{p}{p_{cav}} = \left[\frac{1 + \frac{\gamma - 1}{2} M_d^2 \left(\frac{\omega}{\eta} \right)}{1 + \frac{\gamma - 1}{2} M_d^2} \right]^{\frac{-2(\omega - 1)}{F(\eta - \omega)}} \quad \frac{\gamma}{\gamma - 1} \tag{15}$$

In order to evaluate the local pressure rise, a trajectory of F - κ such as shown in Figure 7 is drawn. For completion of this trajectory, since the value of F and κ at separation and reattachment points are known, only those values of F and κ at the beginning of reattachment should be computed. Using the completed F - κ trajectory local values of $\left(\frac{\omega}{\eta}\right)^{\frac{-2(\omega - 1)}{F(\eta - \omega)}}$ are evaluated at the proper locations in the reattachment zone.

The variation of M_d in the reattachment zone is determined by using Harper [27] analytical solutions of velocity distribution approaching the stagnation poi The velocity of flow approaching the stagnation point depends on vortices Γ_o Γ_1 of inside and outside the stagnating stream lines and angle β as indica in equation (16). Harper's analysis is applicable for incompressible two-dim sional flow but it is assumed that his solution is also applicable for axi-symme reattaching flow.

Harper's solutions are:

$$\text{for} \quad \beta < \frac{\pi}{2}, \quad u_d(x) = \frac{1}{2} (\Gamma_o + \Gamma_1)(L - x) \tan\beta + 0(L - x)$$

$$\beta = \frac{\pi}{2} \quad u_d(x) = -(\Gamma_o + \Gamma_1) \frac{(L - x)}{\pi} \left\{ 2 \ln \left(\frac{L - x}{a_1} \right) + 1 \right\} + 0(L - x) \tag{16}$$

and

$$\beta > \frac{\pi}{2}, \quad u_d(x) = \frac{\pi}{\beta} C (L - x)^{\frac{\pi}{\beta} - 1} + \frac{1}{2} (\Gamma_o + \Gamma_1)(L - x) \tan\beta + 0(L - x)$$

where C and a_1 are constants.

It is noticed that for $\beta = \frac{\pi}{2}$, the inviscid solution of stagnating flow has a logarithmic singularity.

M_a is evaluated by Busemann's integral [30] for a perfect gas, taking the

cavity gas temperature equal to recovery temperature.

Since $$\frac{T_d}{T_e} = 1 + \frac{\gamma - 1}{2} \left(\frac{u_e^2 - u_d^2}{a_e^2} \right)$$

$$\frac{T_d}{T_e} = \frac{T_d}{T_t} \frac{T_t}{T_e} = 1 + \frac{\gamma - 1}{2} \frac{u_e^2}{a_e^2} \left\{ 1 - \left(\frac{u}{u_e} \right)^2 \right\}$$

and $$\frac{T_d}{T_e} = \frac{1 + \frac{\gamma - 1}{2} M_e^2}{1 + \frac{\gamma - 1}{2} M_d^2}$$

it follows

$$M_d^2 = \frac{M_e^2 \, (u_d/u_e)^2}{1 + \frac{\gamma - 1}{2} M_e^2 \left[1 - \left(\frac{u_d}{u_e} \right)^2 \right]}$$

By denoting

$$\frac{u_d}{u_e} = u^*$$

$$M_d^2 = M_e^2 \, u^{*2} / \left\{ 1 + \frac{\gamma - 1}{2} M_e^2 \, (1 - u^{*2}) \right\} \qquad (17)$$

Then the pressure at the reattachment point is

$$\frac{p_r}{p_{cav}} = \left\{ \left(1 + \frac{\gamma - 1}{2} M_{do}^2 \right) \right\}^{\frac{\gamma}{\gamma - 1}}$$

$$= \left\{ \left[\frac{1 + \frac{\gamma - 1}{2} M_e^2}{1 + (1 - u^{*2}) \frac{\gamma - 1}{2} M_e^2} \right] \right\}^{\frac{\gamma}{\gamma - 1}} \qquad (18)$$

η is an empirical efficiency factor of compression relative to that of isentropic process and $\eta \leq 1$. If $\eta = 1$, then compression takes place isentropically.

Numerical Evaluation of Pressure Rise in the Reattachment Zone

The value of $\bar{C}$ is evaluated based on the experimental data of a particular test model of Nicoll [25] as shown in Figure 8. With this model the initial point of rise of pressure and heat transfer is located approximately at the station distance of $1 - \frac{x}{L} = 0.2$. By trial and error, the value of $\bar{C}$ is determined which yields the pressure rise in the reattachment to be in good agreement with experimental data, as seen in Figure 9.

The data of the model and experiment are given:

$$L = 5/8" \qquad D = 1/8" \qquad \frac{L}{D} = 5$$

For helium gas

$$\mathcal{J} = 386 \ \frac{ft}{R^o} \qquad \gamma = 5/3 .$$

The test conditions are $M_\infty = 11$, $T_t = 535^oR$, and $P_t = 400$ psia.

Reynolds number per inch based upon its conditions at the edge of cone boundary layer

$$Re_c/in = 5 . 9 . 10^5$$

Flow parameters at the edge of cone boundary layer are computed by using Reference [31] as follows:

$$M_c = 6.46$$

$$T_c = \frac{535}{1 + \frac{\gamma - 1}{2} M_c^2} = 35.88^oR$$

$$a_c = \sqrt{\gamma g \mathcal{J} T_c} = 144 \sqrt{T_c} = 862 \text{ ft/sec}$$

$$u_c = M_c \cdot a_c = 5560 \text{ ft/sec}$$

$$p_\infty = \frac{p_t}{\left(1 + \frac{\gamma - 1}{2} M_\infty^2\right)^{\frac{\gamma}{\gamma - 1}}} = \frac{400.144}{11,000} = 5.24 \quad \frac{lb}{ft^2}$$

$$p_c = p_\infty \frac{p_c}{p_{t_c}} \frac{p_{t_c}}{p_{t_\infty}} \frac{p_{t_\infty}}{p_\infty} = 5.24 \cdot 7.8 = 40.8 \quad \frac{lb}{ft^2}$$

$$T_\infty = \frac{T_t}{1 + \frac{\gamma - 1}{2} M_\infty^2} = \frac{535}{41.33} = 12.93 \quad {}^\circ R$$

$$\rho_\infty = \frac{p_\infty}{g R T_\infty} = 0.326 \cdot 10^{-4} \quad \frac{lb\ sec^2}{ft^4}$$

$$\rho_c = \rho_\infty / 0.35 = 0.932 \cdot 10^{-4} \quad \frac{lb\ sec^2}{ft^4}$$

$$\nu_c = \frac{u_c}{5.9 \cdot 10^6 \cdot 12} = 7.85 \cdot 10^{-4} \quad \frac{ft^2}{sec.}$$

and

$$\mu_c = \rho_c \cdot \nu_c = 7.31 \cdot 10^{-8} \quad \frac{lb\ sec}{ft^2}$$

The parameters of the cavity flow are:

$$p_{cav} = p_e = 0.85 \cdot p_c \qquad [\text{Ref. 25}]$$

taking

$$p_{e_t} = p_{c_t}$$

$$\frac{p_{cav}}{p_c} = \frac{p_{cav}}{p_{cav_t}} \cdot \frac{p_{cav_t}}{p_{c_t}} \cdot \frac{p_{c_t}}{p_c} = \left(1 + \frac{\gamma - 1}{2} M_e^2\right)^{-2.5} \cdot \left(1 + \frac{\gamma - 1}{2} M_c^2\right)^{2.5}$$

thus

$$M_e = 6.7 \qquad T_e = 33.8\ {}^\circ R,$$

$$\mu_e = 6.85 \cdot 10^{-8} \quad \frac{lb\ sec}{ft^2}, \quad a_e = 840 \quad \frac{ft}{sec}, \quad u_e = 5640 \text{ ft/sec}$$

$$\rho_e = 0.826 \cdot 10^{-4} \quad \frac{lb\ sec^2}{ft^4}$$

and

Assuming that the reattachment begins at $x = 0.8\ L$, [25], and at this position $u^* = 0.587$, the pressure ratio at the reattachment point is

$$\frac{p_r}{p_{cav}} = \left\{ \left[\frac{1 + \frac{\gamma - 1}{2} M_e^2}{1 + (1 - u^{*2}) \frac{\gamma - 1}{2} M_e^2} \right]^{\frac{\gamma}{\gamma - 1}} \right\} = \left\{ \cdot\ 2.65 \right.$$

$$\frac{P_R}{P_{cav}} = \frac{P_R}{P_e} \qquad \frac{P_c}{P_{cav}} = \frac{1.5}{0.85} = 1.76$$

From Figure 4 of Reference [25], [also Figure 9 of this Report], it is estimated that

$$\text{thus} \quad \xi = 0.665 \tag{19}$$

This result shows that the isentropic compression occurs upstream of reattachment.

For the selected model configuration, it is likely that $\beta < \frac{\pi}{2}$ thus the velocity distribution in the reattachment zone is from equation (16).

$$u_d(x) = \frac{1}{2} \left(\Gamma_o + \Gamma_1 \right) (L - x) \tan \beta$$

A small term of 0 (L-x) of equations (16) is neglected).

Assuming that $\frac{1}{2} \left(\Gamma_o + \Gamma_1 \right) \tan \beta = C_1$

Then $u_d(x) = C_1 (L - x)$

This unknown constant C_1 is determined by matching with the experimental data at the beginning of reattachment, i.e., at the position of $L - x = 0.2\ L = \frac{1}{96}$ as,

$$C_1 = 3.17.10^5 \quad \frac{\text{ft.}}{\text{sec. ft.}}$$

Hence

$$u_d = 3.17.10^5 (L - x) \tag{20}$$

Since

$$\frac{T_d}{T_e} = 1 + \frac{\gamma - 1}{2} M_e^2 \left(1 - u^{*2} \right)$$

$$a_d = 144 \sqrt{T_a} = 2750 \text{ ft/sec}$$

and $M_d = u_d / a_d$

$$M_d = 1.15 . 10^2 (L - x) \tag{21}$$

For the trajectory of F - κ , the following values of F and κ are taken from Reference [5] at the separation and reattachment points, namely,

$F_S = 2.85$ $\qquad$ $\kappa_S = 0.63$

$F_R = .59$ $\qquad$ $\kappa_R = 0.693$

The values of F and κ at reattachment point are those of Blasius flow. At the point of beginning of reattachment.

$$\kappa_o = 1 - \frac{1 - \kappa_S}{\sqrt{1 + \frac{2(1 - \kappa_S^2)}{A}\bar{C}\,\frac{x}{\ell}}}$$

By the method of trial and error, the values of $\bar{C}$ and κ_o are determined.

Taking $\bar{C} = 15$,

$$\ell = \frac{1.25}{12} \text{ ft. and } \quad x = 0.8.L,$$

it becomes

$$\kappa_o = 0.83$$

Figure 7 shows the completed trajectory, with the local values of F and along the reattachment distance. Since local values of F and κ are known as shown in Table 1 the local values of $\left(\frac{\omega}{\eta}\right)^{\frac{-2(\omega - 1)}{F(\eta - \omega)}}$ and pressure in the reattachment zone are computed.

Table 1
Reattachment Pressure Rise (Computed)

$1 - \frac{x}{L}$	κ	F	$\left(\frac{\omega}{\eta}\right)^{\frac{-2(\omega - 1)}{F(\eta - \omega)}}$	$\frac{\gamma - 1}{2} M_d^2$	$\frac{p}{p_{cav}}$	$\frac{p}{p_c}$
0.2	0.83	2.85	1	0.480	1	0.85
0.16	0.802	2.6	1.0255	0.3072	1.0151	0.8628
0.12	0.775	2.35	1.0544	0.1728	1.0202	0.8671
0.1	0.765	2.23	1.0668	0.120	1.0180	0.8653

As seen in Figure 9, the computed values of pressure are in excellent agreement close to upstream half distance in the reattachment zone. This result confirms that $\bar{C} = 15$ is an acceptable value in the region of upstream reattachment zone of a laminar cavity flow which Glick [5] used successfully for the region of reattachment zone downstream of shock impingement.

From Figure 9 it is also noticed that the measured value of pressure reac close to its cone value at point A which is located at three-fourth downstream distance of the reattachment zone. This value of pressure corresponds approximately to that computed by isentropic compression, with the M_d at that positio multiplied by the average value of $\zeta_{av} = \frac{1 + 0.665}{2} = 0.8325$ between separation and reattachment.

3. Heat Transfer in the Reattachment Zone

At present no analysis for the heat transfer at the reattachment point is available. However, since the process of reattachment is similar to that of stagnation, for the evaluation of reattachment heat transfer, the known stagnation heat transfer formula may be referred. Therefore, it is of interest to compare the empirical data of reattachment heat transfer with those predicted by the stagnation heat transfer equation.

At hypersonic speed, Chung and Viegas [15] employed the following semi-empirical formula of average heat transfer in a reattachment region of $0 < \frac{L - x}{L} < 1$ based upon the stagnation heat transfer analysis of Lees [33] for highly cooled wall, namely

$$q_{w.r} \simeq 2^{\frac{3}{2}} Pr^{-\frac{2}{3}} \sqrt{\rho_t \mu_t} \sqrt{\frac{u_d}{L_R}} (H_t - H_w) \left(0.76 + 1.411 \frac{p_e}{p_t}\right) \tag{22}$$

This equation is applicable for two-dimensional flow with $\beta \simeq 45^{\circ}$ and also for $0.1 \leq \frac{p_e}{p_t} \leq 0.5$ where H is total enthalpy.

If this equation is assumed to be applicable for the axial symmetric flow, $\frac{p_e}{p_R} = \frac{1}{1.76} = 0.57$ and for small area of reattachment similar to Nicoll's experimental model [Figure 8b. Ref. [25]], since

$$q = h (T_w - T_{aw})$$

equation (22) may be written

$$h_R = \frac{H_t - H_w}{T_w - T_{aw}} \; 0.69 \sqrt{\rho_R \mu_R} \sqrt{\frac{u_d}{L_R}}$$

assuming

$$\frac{\mu_R}{\mu_e} = \frac{T_R}{T_e}, \qquad \frac{\rho_R}{\rho_e}\frac{\mu_R}{\mu_c} = \frac{p_R}{p_e}\frac{T_e}{T_R}\frac{T_R}{T_e} = \frac{p_R}{p_e}$$

and at the reattachment where $\zeta = 0.665$ taking $T_R \approx T_{aw}$, it becomes

$$h_R = 0.945 \sqrt{\rho_e \mu_e} \sqrt{\frac{u_d}{L_R}} c_p \tag{23}$$

For cone

$$h_c = St_c \cdot \rho_c \cdot u_c \cdot c_p$$

and at the reattachment point,

$$Re_c = 5{,}9.10^5 \left(1.25 + \frac{5}{8}\right) = 1.108.10^6$$

For this Reynolds number, from Figure 2, Reference [25],

$$St \approx 5.10^{-4}$$

and

$$\rho_c u_c = 0.932 \cdot 10^{-4} \cdot c_p$$

Therefore

$$h_c = 2.64.^{10^{-4}} \cdot c_p. \tag{24}$$

From equation (23) and (24). For $u_d = 0.587 \cdot 5640 = 330$ ft/sec.

$$\frac{h_R}{h_c} \approx \frac{0.505}{L_R} \tag{25}$$

Thus h_R/h_c is inversely proportional to $\sqrt{L_R}$.

Chung and Viegas formula yields

(a) For $L_R = 0.008 \cdot L = 0.008 \frac{5}{8} \frac{1}{12} = 0.00417$ ft

$$\frac{h_R}{h_c} = 7.82$$

(b) For $L_R = 0.2 \cdot L = 0.2 \cdot \frac{5}{8} \cdot \frac{1}{96}$ ft.

$$\frac{h_R}{h_c} = 4.95$$

(26)

L_R of Case (a) corresponds to the measured value of L_R (Ref. [15]for $\beta \approx 45^\circ$ and L_R of Case (b) is that of the measured $L_R = 0.2 \cdot L$ by Nicoll [25].

By comparing these average values of h_R/h_c of equation (26), with Nicoll's (Figure 8b, Ref. [25]) average value of $h_R/h_c = 2.63$.

Case (a) $(h_R/h_c)_{\substack{\text{Chung}\\\text{Viegas}}} \Big/ \left(\frac{h_R}{h_c}\right)_{\text{Nicoll}} = 2.975 \approx 3$

Case (b) $(h_R/h_c)_{\substack{\text{Chung}\\\text{Viegas}}} \Big/ \left(\frac{h_R}{h_c}\right)_{\text{Nicoll}} = 1.88 \approx 2$

Hence, Chung-Viegas' semi-empirical formula for reattachment heat transfer predicts higher heat transfer values than those obtained by experiment.

In order to more accurately establish the prediction of heat transfer in the reattachment zone, the distribution of velocity u_s along the reattachment surface $\bar{s}$ and the velocity gradient at the reattachment point must be determined. Because the flow process at the reattachment point is complex, the reattachment velocity gradient is determined semi-empirically, but u_s, the potential flow velocity along $\bar{s}$ downstream of reattachment point, is computed, using Squire's model of cavity flow involving a core, and its surrounding boundary layer as shown in Figures 1 and 2.

Although the viscosity is responsible for the development of the motion in the cavity, within the core the viscosity effect is small. Thus, the flow along the outside border line which is also the border line of the boundary laryer is assumed to be inviscid. Then, u_s the potential velocity along the wall, can be computed along this border line of the boundary layer.

Hence, by simplicity assuming the flow motion in the reattachment zone is incompressible, the following Bernoulli's equation is applicable in the reattachment zone.

$$\frac{p_R}{\rho} = \frac{p}{\rho} + \frac{u_s^2}{2}$$

Then

$$\frac{u_{\bar{s}}}{u_d} = \sqrt{\frac{p_R - p}{\rho u_d^2/2}} = \sqrt{\frac{p_R - p}{q_d}} \tag{27}$$

where

$$q_d = \frac{\rho u_d^2}{2}$$

The heat transfer in the region of stagnation point of cold blunt nose is give by Lees [32]. Writing this equation for u_d along the dividing stream line whic may be considered the upstream velocity of reattachment, similar to upstream free stream velocity approaching stagnation point, one obtains

$$\frac{q_w}{q_{w_R}} = \frac{\frac{1}{2}\left(p/p_R\right) \frac{u_{\bar{s}}}{u_d} r_o}{\left[\int_o^{\bar{s}} \frac{p}{p_R} \frac{u_{\bar{s}}}{u_d} r_o^2 \, d\bar{s}\right]^{\frac{1}{2}}} \quad \frac{1}{\sqrt{\frac{1}{u_d}\left(\frac{du_{\bar{s}}}{d\bar{s}}\right)_{\bar{s}=0}}} \tag{28}$$

where r_o is radius of cross section of body of revolution. Equation (28) is a function of u_d because the heat transfer process in the reattachment zone, similar to the case of pressure rise in the reattachment zone can be formulated by the flow properties along the dividing stream line.

Thus

$$\sqrt{\frac{1}{u_d}\left(\frac{d\,u_{\bar{s}}}{d\,\bar{s}}\right)_{\bar{s}=0}} = \text{constant} = C_2$$

the constant is to be evaluated.

Equation (28) reduces to

$$\frac{q_w}{q_{w_R}} = \frac{\frac{1}{2}\left(p/p_R\right)\sqrt{\frac{p_R - p}{q_d}} \cdot r_o}{C_2\left[\int_o^{\bar{s}} \frac{p}{p_R}\sqrt{\frac{p_R - p}{q_d}}\, r_o^2 \, d\bar{s}\right]^{\frac{1}{2}}} \tag{29}$$

Hence by knowing pressure distribution along the dividing stream line within the reattachment zone for a given geometry, the heat transfer in the reattachment zone can be computed if C_2 is determined empirically.

Numerical Evaluation of Heat Transfer in the Reattachment Zone

Chung and Viegas [15] found the stream function by solving the reattachment flow as incompressible two-dimensional inviscid but rotational as

$$\frac{\psi\left[\frac{\bar{s}}{L_R}\ \frac{L-x}{L_R}\right]}{u_d\ L_R} = \frac{\coth\ \lambda L_R}{\lambda L_R}\left[\sinh\ \lambda L_R\ \left(\frac{L-x}{L_R}\right)\right]$$

$$+\ \frac{1-\cosh \lambda L_R\ \left(\frac{L-x}{L_R}\right)}{\lambda L_R} - \frac{\frac{L-x}{L_R}}{\lambda L_R}\exp\left(-\lambda L_R\ \frac{\bar{s}}{L_R}\right.$$

$$-2\sum_{n=1}^{\infty}\frac{\lambda L_R\left[\sin n\pi\left(\frac{L-x}{L_R}\right)\right]}{n\pi\left[(n\pi)^2+(\lambda L_R)^2\right]}\exp\left[-\sqrt{(n\pi)^2+(\lambda L_R)^2}\ \frac{\bar{s}}{L_R}\right]$$

where λ is a parameter and its numerical value is $\lambda = \frac{1}{2.222}\ \frac{Re_L}{L}$

and $R_{e_L} = \frac{u_e L}{\nu_e}$

Since $u_{\bar{s}} = \frac{\partial \psi}{\partial\left(\frac{L-x}{L_R}\right)}$

the velocity gradient at the reattachment point is

$$\left[\frac{1}{u_d L_R}\ \frac{\partial}{\partial\left(\frac{\bar{s}}{L_R}\right)}\ \frac{\partial \psi}{\partial\left(\frac{L-x}{L_R}\right)}\right]_{\substack{\frac{L-x}{L_R}\to 0 \\ \frac{\bar{s}}{L_R}\to 0}} = 1 + 2\sum_{n=1}^{\infty}\frac{\lambda L_R}{\sqrt{(n\pi)^2+(\lambda L_R)^2}}$$

or $$\left.\frac{du_{\bar{s}}}{d\bar{s}}\right|_{\substack{\bar{s}\to 0 \\ x\to L}} = \frac{u_d}{L_R}\left[1+2\sum_{n=1}^{\infty}\frac{1}{\sqrt{1+\left(\frac{\pi}{\lambda L_R}\right)^2 n^2}}\right]$$

Now with sufficiently large n value, say n_1

$$1 + \left(\frac{\pi}{\lambda L_R}\right)^2 n^2 \rightarrow \left(\frac{\pi}{\lambda L_R}\right)^2 n^2$$

hence the series for terms larger than n_1 become

$$2 \sum_{n_1}^{\infty} \frac{\lambda L_R}{\pi} \frac{1}{n} = \frac{2 \lambda L_R}{\pi} \sum_{n_1}^{\infty} \frac{1}{n} \rightarrow \infty$$

or

$$\left.\frac{du_s}{d\bar{s}}\right|_{\substack{\bar{s} \rightarrow 0 \\ x \rightarrow L}} \rightarrow \infty$$

This singularity of velocity gradient at the reattachment is physically impossible. As previously mentioned Burggraf's [13] analysis leads to the reattachment heat flux to square root singularity.

At present no other analysis of reattachment velocity gradient is available therefore its value is evaluated empirically from experimental data of Nicoll [25] with the test model sketched in Figure 8.

Since with this model, the initial point of pressure and heat transfer coinc approximately at $1 - \frac{x}{L} = 0.2$, it is simple to correlate the pressure and heat transfer in the reattachment zone.

Rewriting equation (29) by cone values of pressure,

$$\frac{q_w}{q_{w_R}} = \frac{\frac{1}{2} \frac{p}{p_c} \frac{p_c}{p_R} \sqrt{\frac{p_c}{q_d}\left(\frac{p_R}{p_c} - \frac{p}{p_c}\right)}\, r_o}{C_2 \left[\int_0^{\bar{s}} \frac{p}{p_c} \frac{p_c}{p_R} \sqrt{\frac{p_c}{q_d}\left(\frac{p_R}{p_c} - \frac{p}{p_c}\right)}\, r_o^2 \, d\bar{s}\right]^{\frac{1}{2}}} \qquad (30)$$

The heat transfer coefficient ratio is,

$$\frac{h}{h_c} = \frac{h}{h_R} \frac{h_R}{h_c} = \frac{q_w (T_w - T_{aw})_R}{q_{w_R} (T_w - T_{aw})} \frac{h_R}{h_c}$$

(31)

The local value of h_R/h_c is estimated by multiplying a factor of 1.15 to the average value of h/h_c in the small area at the reattachment point, Figure 8b, Ref.[25] .

Thus, $$\frac{h_R}{h_c} \simeq 1.5 \left(\frac{h_{R\,av}}{h_c}\right) = 1.15 \cdot 2.63 \approx 3.0$$

Since, $$T_d = T_e\left[1 + \frac{\gamma-1}{2} M_e^2 \left\{1-u^{*2}\right\}\right] = 365^{\circ}R$$

and $$\rho_d = \frac{p_d}{gRT_d} = \frac{42 \cdot 0.85}{32.2 \cdot 386 \cdot 365} = 0.792.10^{-5} \quad \frac{lb\ sec^2}{ft^4}$$

$$u_d = 0.587.5640 = 3300 \quad ft/sec$$

and $$q_d = \frac{\rho_d u_d^2}{2} = 43$$

it becomes $p_c/q_d \approx 1.$

The value of C_2 is evaluated by equation (30) at a position of $1 - \frac{x}{L} = 0.04$, where $\frac{h}{h_c} = 1.34$ or $\frac{q_w}{q_{wr}} = 0.446.$

The values of denominator and nominator of equation (30) excluding C_2 are listed in Table 2.

Table 2

Computed Values of Equation 30

$1 - \frac{x}{L}$	$\frac{1}{2}\frac{p}{p_c}\frac{p_c}{p_R}\sqrt{\frac{p_c}{q_d}\left(\frac{p_R}{p_c} - \frac{p}{p_c}\right)}\, r_o$	$\int_o^{\bar{s}} \frac{p}{p_c}\frac{p_c}{p_R}\sqrt{\frac{p_c}{q_d}\left(\frac{p_R}{p_c} - \frac{p}{p_c}\right)}\, r_o^2 d\bar{s}$
0.2	$0.3425.10^{-2}$	$2.7985.10^{-6}$
0.16	$0.3525.10^{-2}$	$2.5335.10^{-6}$
0.12	$0.365.10^{-2}$	$2.326.10^{-6}$
0.08	$0.406.10^{-2}$	$1.965.10^{-6}$
0.04	$0.4515.10^{-2}$	$1.54.10^{-6}$
0	0	0

Since $1 - \frac{x}{L} = 0.04$,

it follows $C_2 = (1.54.10^{-6})^{\frac{1}{2}} = \frac{0.4515.10^{-2}}{0.446} = 1.01.10^{-2}$

$$C_2 = 8.15 \qquad (32)$$

or $$\frac{1}{u_d}\left(\frac{du_{\bar{s}}}{d\bar{s}}\right)_{\bar{s}=0} = 66.5$$

Denoting d = 2D, the stagnation velocity gradient,

$$\frac{d}{u_d}\left(\frac{du_{\bar{s}}}{d\bar{s}}\right)_{\bar{s}=0} = \frac{2}{8}\,\frac{1}{12}\,66.5 = 1.39 \approx \frac{\pi}{2}$$

From Figure 7-16, Ref. [33] it is seen that this value of stagnation veloci gradient corresponds to that of blunt-nosed body for incompressible flow as we as to Newtonian flow for supersonic flow.

Finally, the local values of h is determined from equation (31). Since th ratio of local value of $\frac{(T_w - T_{aw})_R}{T_w - T_{aw}}$ is not known, it is necessary to evalu this ratio first.

At reattachment, $1 - \frac{x}{L} = 0$, $\frac{(T_w - T_{aw})_R}{T_w - T_{aw}} = 1$ and at the initial point of reattachment, i.e., at $1 - \frac{x}{L} = 0.2$, $\frac{q_w}{q_{wR}} = 0.251$ and $\frac{h}{h_c} = 0.35$ (Figure 8b, Reference [25]), thus from equation (31) $\frac{(T_w - T_{aw})_R}{T_w - T_{aw}} = 0.4$

Assuming a linear variation of $\frac{(T_w - T_{aw})_R}{T_w - T_{aw}}$ in the reattachment distance, thus drawing a straight line which has its initial and end values of $\frac{(T_w - T_{aw})_R}{T_w - T_{aw}}$ equal 0.465 and 1, as seen in Figure 10, the local values of $\frac{(T_w - T_{aw})_R}{T_w - T_{aw}}$ are determined as shown in Table 3 or Figure 10.

Then from equation (31) local values of $\frac{h}{h_c}$ are computed as indicated in Table 3 and Figure 10.

Table 3

Computed Values of Equation (31)

$1 - \frac{x}{L}$	q_w / q_{wR}	$(T_w - T_{aw})_R / (T_w - T_{aw})$	h/h_c
0.2	0.251	0.465	0.35
0.16	0.271	0.57	0.462
0.12	0.292	0.676	0.59
0.08	0.354	0.782	0.828
0.04	0.446	0.89	1.19
0	1	1	3

The comparison of computed values of h/h_c with those measured shows good agreement among them, as seen in Figure 10. Therefore, it appears that the assumed condition of incompressible flow prevails in the reattachment zone.

In order to confirm this, $M_{\bar{s}}$ and density ratio of $\frac{\rho_{\bar{s}}}{\rho_d}$ are computed with the temperature distribution shown in Table 3.

Since

$$\frac{u_{\bar{s}}}{u_d} = \frac{u_{\bar{s}}}{a_d} \frac{a_d}{u_d} = \frac{M_{\bar{s}}}{M_d}$$

and

$$M_d = 1.212, \text{ with test condition } M_{\bar{s}} = 0.812 - 0.98 < 1$$

in the reattachment zone.

Then

$$\frac{\rho_{\bar{s}}}{\rho_d} = \frac{p_{\bar{s}}}{p_d} \frac{T_d}{T_{\bar{s}}} = 1.11$$

in the range near 80% of the reattachment zone extending from the initial point of reattachment to downstream distance.

These figures of $M_{\bar{s}}$ and $\frac{\rho_{\bar{s}}}{\rho_d}$ may justify the assumed condition of incompressible flow in the reattachment zone.

Assuming that the known stagnation heat transfer equation for blunt body is applicable for the reattachment, the following formula [34] is used.

$$q_{w_R} = f_2 \sqrt{\left(\frac{du_{\bar{s}}}{d\bar{s}} \right)_{\bar{s}=0} \rho_d \mu_d} \cdot c_p \, (T_w - T_{aw}) \tag{33}$$

where $f_2 = 0.57 . Pr^{-0.6}$ for two-dimensional flow

$f_2 = 0.763 . Pr^{-0.6}$ for axially symmetric flow

The equation (33) is written by flow property along the dividing stream line at the beginning of reattachment, i.e., $\rho_d \mu_d$ (For stagnation heat transfer for blunt nose exposed free stream, this term is $\rho_\infty \mu_\infty$).

Since $\rho_d \mu_d = \rho_e \mu_e$ and if one assumes a linear relation of $\mu - T$ equation (33) becomes

$$h_R = f_2 \, c_p \sqrt{\rho_e \mu_e} \sqrt{\left(\frac{du_{\bar{s}}}{d\bar{s}} \right)_{\bar{s}=0}} \tag{34}$$

This equation expresses h_R based upon the flow condition at the outer edge of viscous layer.

Because $h_c = St_c . p_c . u_c . c_p$ as before,

$$\frac{h_R}{h_c} = \frac{f_2}{St_c} \frac{\sqrt{\rho_e \mu_e}}{\rho_c u_c} \sqrt{\left(\frac{du_{\bar{s}}}{d\bar{s}} \right)_{\bar{s}=0}} \tag{35}$$

For the test condition of the model sketched in Figure 8,

$$(\rho_e \mu_e)^{\frac{1}{2}} = (0.826.10^{-4} . 6.85.10^{-8})^{\frac{1}{2}} = 2.377.10^{-6} \left(\frac{lb^2 sec^3}{ft^6} \right)^{\frac{1}{2}}$$

$$\rho_c u_c = 0.932.10^{-4} . 5560 = 0.52 \quad \frac{lb. sec.}{ft^3}$$

$St_c = 5.10^{-4}$ referring to the cone value at the reattachment point, and

since $\frac{1}{u_d}\left(\frac{du_{\bar{s}}}{d\bar{s}}\right)_{\bar{s}=0} = 66.5$, $\left(\frac{du_{\bar{s}}}{d\bar{s}}\right)_{\bar{s}} = 22.10^4$

from equation (35)

$$\frac{h_R}{h_c} = f_2 \frac{2.377.10^{-6}}{5.10^{-4} \cdot 0.52} \sqrt{22.10^4} = f_2 \cdot 4.3$$

In helium $Pr^{-0.6} = (0.68)^{-0.6} = 1.26$

$f_2 \approx 0.72$ for two-dimensional flow

$f_2 \approx 0.96$ for axially symmetric flow

Finally

$\frac{h_R}{h_c} = 3.12$ for two-dimensional flow

$\frac{h_R}{h_c} = 4.15$ for axially symmetric flow

but $\frac{h_R}{h_c} \simeq 3.0$ from experiment.

From these results, it appears that reattachment heat transfer may be predicted in a good agreement with experimental data by using stagnation heat transfer equation for blunt nosed body assuming reattachment heat transfer is essentially a two-dimensional process, because the assumption of axially symmetric flow could lead to higher value of reattachment heat transfer.

Actual reattachment process is very complicated involving geometry of reattachment surface, angle β , reverse flow, etc. Hence further study is needed to clarify the difference between the reattaching and stagnating flow processes involving the velocity gradient parameter at the reattachment point.

4. Discussions

The distributions of pressure and heat transfer of cavity flow are affected by the geometry of cavity; i.e., by L/D, the ratio of length to depth. As shown in Figure 11 and 12, the pressure rises immediately after separation and continues to rise in the whole region of the cavity if L/D is large, say L/D = 10, but the heat transfer rates remain constant except in the narrow region of reattachment for L/D = 40/3. On the other hand, as shown also in Figure 11 and 13, if L/D is smaller, say L/D = 5, the pressure remains constant upstream of reattachment, only rising sharply in the reattachment zone, but at the same L/D the heat transfer rate reaches minimum at the center of cavity and rises rapidly approaching the reattachment point. These behaviors of pressure and heat transfer appear strongly influenced by the recirculating flow characteristics depending upon the depth of its cavity. Because the initial points of rise of pressure and heat transfer must be known for the prediction of reattachment process, the location of the initial point of reattachment must be determined for a given L/D.

Burggraf's [13] paper which considers the various depths of the cavity was obtained at a late stage in the preparation of this report. Thus, no investigation of these reattachment behaviors has been made using Burggraf's analysis.

It is found that Glick's method [5] for computation of reattachment flow involving shock interaction is applicable for the cavity flow. Also the semi-empirical average mixing rate correlation parameter $\bar{C}$ is the same for these two flows. But it is still unknown whether Glick's analysis is also applicable to other types of separated and reattached flows such as caused by forward as well as reward facing steps, corners and ramps, etc.

An analytical study is desirable in order to evaluate the reattachment velocity radient parameter for arbitrary geometry of reattachment surface, angle β etween dividing stream line and reattachment wall and reverse flow etc.

5. Conclusions

An investigation of the cavity flow based on Chapman-Squire type physical model referring to the experimental data of a particular limited model at free stream Mach number 11, leads to the following conclusions.

Predictions of pressure rise and heat transfer in the reattachment zone can be made by flow conditions on the dividing stream line.

Pressure rise can be computed by Glick's procedure of analysis with an average mixing rate correlation function $\overline{C} = 15$ in the mixing zone upstream of reattachment employing Crocco-Lees' mixing theory. Up to upstream half zone of reattachment, the pressure rise takes place by isentropic compression, but approaching reattachment point, due to compressibility, viscosity, geometry of reattachment surface, reverse flow, etc. the pressure rise is less than that of isentropic compression.

An estimation of reattachment heat transfer may be made by using the known stagnation heat transfer equation for blunt nosed body.

However, additional experimental data of pressure and heat transfer distribution in the reattachment zone of various geometrical configurations, as well as the analytical prediction of reattachment heat transfer are needed to clarify completely the reattachment heat transfer in the cavity zone.

References

1. Tanner, M. "Zur Bestimmung des Totwasserwiderstaudes mit Anwendung auf Totwasser hinter Keilen." Mitteilungen aus dem Max-Planck Institut für Strömungsforschung und der Aerodynamischen Versuchsanstalt, No. 31, 1964.

2. Chapman, D. R. "Laminar Mixing of a Compressible Fluid," NACA Rept. 958, 1950.

3. Chapman, D. R. "A Theoretical Analysis of Heat Transfer in Regions of Separated Flow," NACA TN 3792, 1956.

4. Crocco, L. and Lees, L. "A Mixing Theory for the Interaction Between Dissipative Flows and Nearly Isentropic Streams," Journal of the Aeronautical Sciences. Vol. 19, No. 10, pp. 649-676. Oct. 1952.

5. Glick, H. S. "Modified Crocco-Lees Mixing Theory for Supersonic Separated and Reattaching Flows," Hypersonic Research Project, Memo No. 53, May 1960. Guggenheim Aeronautical Laboratory, California Institute of Technology. Also Journal of Aerospace Sciences, Oct. 1962, pp. 1238-49.

6. Bloom, M. H. "On Moderately Separated Viscous Flows," Journal of Aerospace Sciences, Vol. 28, No. 4, April 1961, pp. 339-340.

7. Chapman, D. R., Kuehn, D. M., and Larson, H. K. "Investigation of Separated Flows in Supersonic and Subsonic Streams with Emphasis on the Effect of a Transition," NACA Rept. 1356, 1958.

8. Korst, H. H., Page, R. H., and Childs, M. E. "A Theory for Base Pressures in Transonic and Supersonic Flow," University of Illinois, ME-TN-392-2, Dec. 1959.

9. McDonald, H. "Turbulent Shear Layer Re-attachment with Special Emphasis on the Base Pressure Problem," The Aeronautical Quarterly, Vol. XV, Aug. 1964, pp. 247-280.

10. Squire, H. B. "Note on the Motion Inside a Region of Recirculation (Cavity Flow)," Journal of the Royal Aeronautical Society, 60, March 1956, pp. 203-205.

11. Mills, R. D. "On the Closed Motion of a Fluid in a Square Cavity," Journal of the Royal Aeronautical Society, Feb. 1965, p. 116.

12. Batchelor, G. "On Steady Laminar Flow with Closed Stream Lines at Large Reynolds Number," Journal.Fluid Mechanics, Vol. 1, part 1, 1956, p. 177.

13. Burggraf, O. R. "A Model of Steady Separated Flow in Rectangular Cavities at High Reynolds Number," Proceedings of the 1965 Heat Transfer and Fluid Mechanics Institutes, Stanford University Press, 1965, p. 190.

14. Burggraf, O. R. "Analytical and Numerical Studies of the Structure of Steady Separated Flows," Journal.Fluid Mechanics, Vol. 24, part 1, pp. 113-151, 1966.

15. Chung, P. M., and Viegas, J. R. "Heat Transfer at the Reattachment Zone of Separated Laminar Boundary Layers," NASA D-1072, Sept. 1961.

16. Carlson, W. O. "A Solution for Heat Transfer in Laminar Separated and Wake Flow Regions," General Electric, R 595SD356, 1959. Also paper presented at 1959 Heat Transfer and Fluid Mechanics Institute held at University of California, Los Angeles, California, June 11-13, 1959, Stanford University Press, Stanford, California, pp. 140-155.

. Korst, H. H. "Dynamics and Thermodynamics of Separated Flows." Presented at the Symposium on "Single-and Multi-Component Flow Processes." May 1, 1964, Rutgers Engineering Centennial. Rutgers--The State University, New Brunswick, New Jersey.

. Roskho, A. "Some Measurements of Flow on a Rectangular Cutout," NACA TN 3488, 1955.

. Tani, I., Iuchi, M., and Komada, H. "Experimental Investigation of Flow Separation Associated with a Step on a Groove, "Aeronautical Research Institute, University of Tokyo, Rept. No. 364, April, 1961.

. Maull, D. J. and East, L. F. "Three-Dimensional Flow in Cavities," Journal.Fluid Mechanics, Vol. 16, 1963, pp. 620-632.

. Fox, J. "Flow Regimes in Transverse Rectangular Cavities," Proceedings of the 1965 Heat Transfer and Fluid Mechanics Institute, Stanford University Press, 1965, pp. 230-241.

. Charwat, A. F., Roos, J. N., Dewey, F. C., Jr., and Hitz, J. A. "An Investigation of Separated Flows," Journal of the Aerospace Sciences, No. 6 and 7, June and July 1961.

. Larson, H. K. "Heat Transfer in Separated Flows," Journal of the Aerospace Sciences, Nov. 1959, pp. 731-38.

. Bogdonoff, S. M. and Vas, I. E. "Some Experiments on Hypersonic Separated Flows," ARS J., Vol. 32 (11), 1962, p. 1564.

. Nicoll, K. M. "A Study of Laminar Hypersonic Cavity Flows," AIAA Journal, Vol. 2, No. 9, Sept. 1964, pp. 1535-41.

26. Denison, M. R. and Baum, E. "Compressible Free Shear Layer with Finite Initial Thickness," AIAA Journal, Vol. 1, No. 2, Feb. 1963, p. 342.

27. Harper, J. F. "On the Boundary Layers in Two-Dimensional Flow with Vorticity," Journal of Fluid Mechanics, Vol. 17, Part I, Sept. 1963, pp. 141-153.

28. Tani, I. "Experimental Investigation of Flow Separation Over a Step," Grenzschichtforschung, IUTAM - Symposium, Freiburg (Br.) 1957. Herausgegeben von H. Görtler, Springer-Verlag 1958, pp. 377-386.

29. Crocco, L. "Considerations on the Shock-Boundary Layer Interaction," Proceedings of the Conference on High-Speed Aeronautics, Polytechnic Institute of Brooklyn. Brooklyn, New York, Jan. 20-22, 1955.

30. Busemann, A. "Gasströmung mit laminarer Grenzschict entlang einer Platte," ZAMM, Bd. 15 Heft 1/2. Feb. 1935, pp. 23-25.

31. Henderson, A. and Braswell, D. O. "Charts for Conical and Two-Dimensional Oblique-Shock Flow Parameters in Helium at Mach Numbers from about 1 to 100," NASA TN D-819, June 1961.

32. Lees, L. "Laminar Heat Transfer Over Blunt-Nosed Bodies at Hypersonic Flight Speeds," Jet Propulsion, April 1956, pp. 259-268.

33. Truitt, R. W. Hypersonic Aerodynamics. New York: The Ronald Press Co., 1959.

34. Truitt, R. W. Fundamentals of Aerodynamic Heating. New York: The Ronald Press Co., 1960, pp. 168-169.

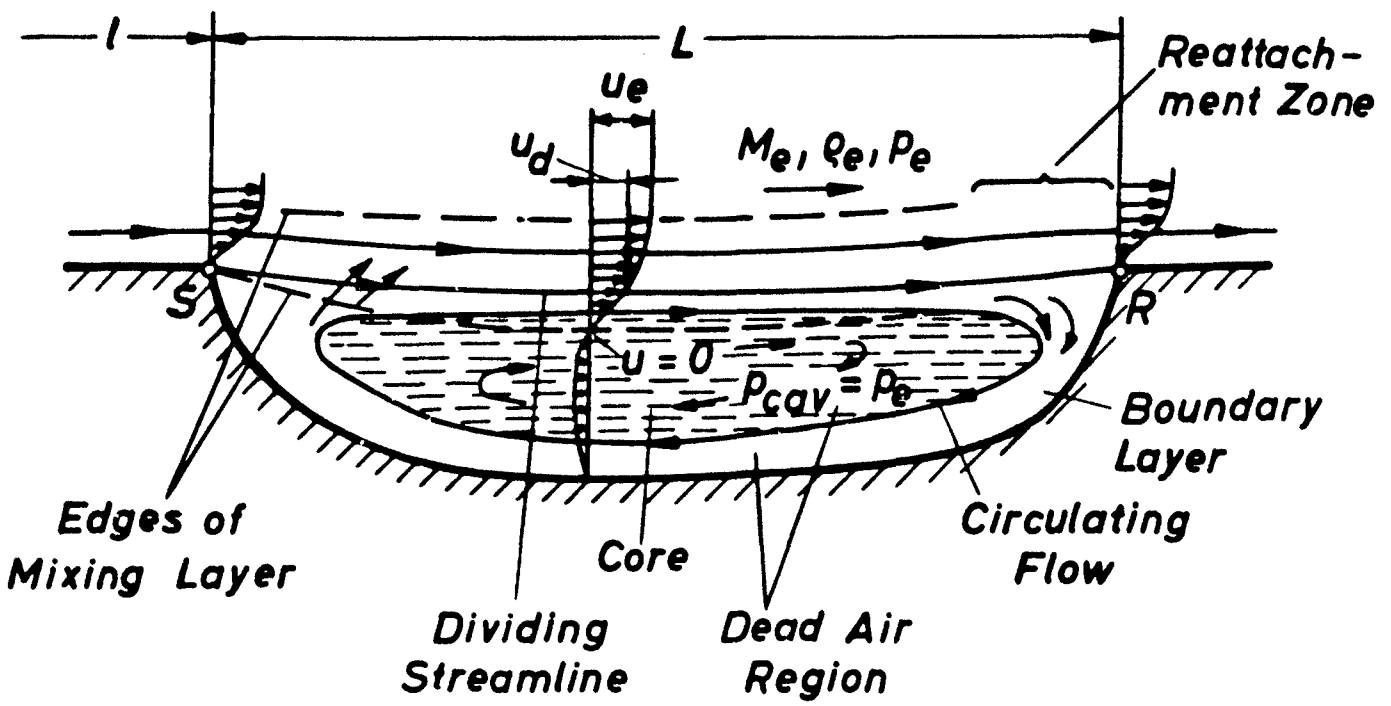

Figure 1 Separated and Reattached Cavity Flow Field

(Vertical Scale Expanded)

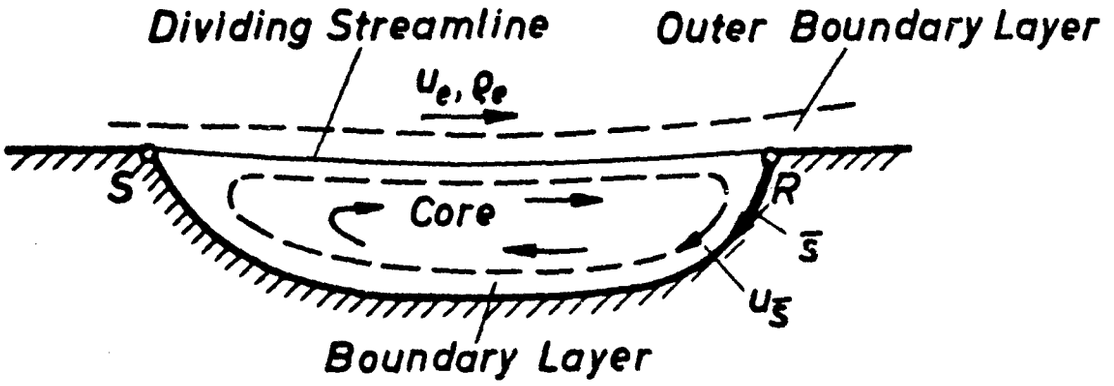

Figure 2 Recirculating Cavity Flow

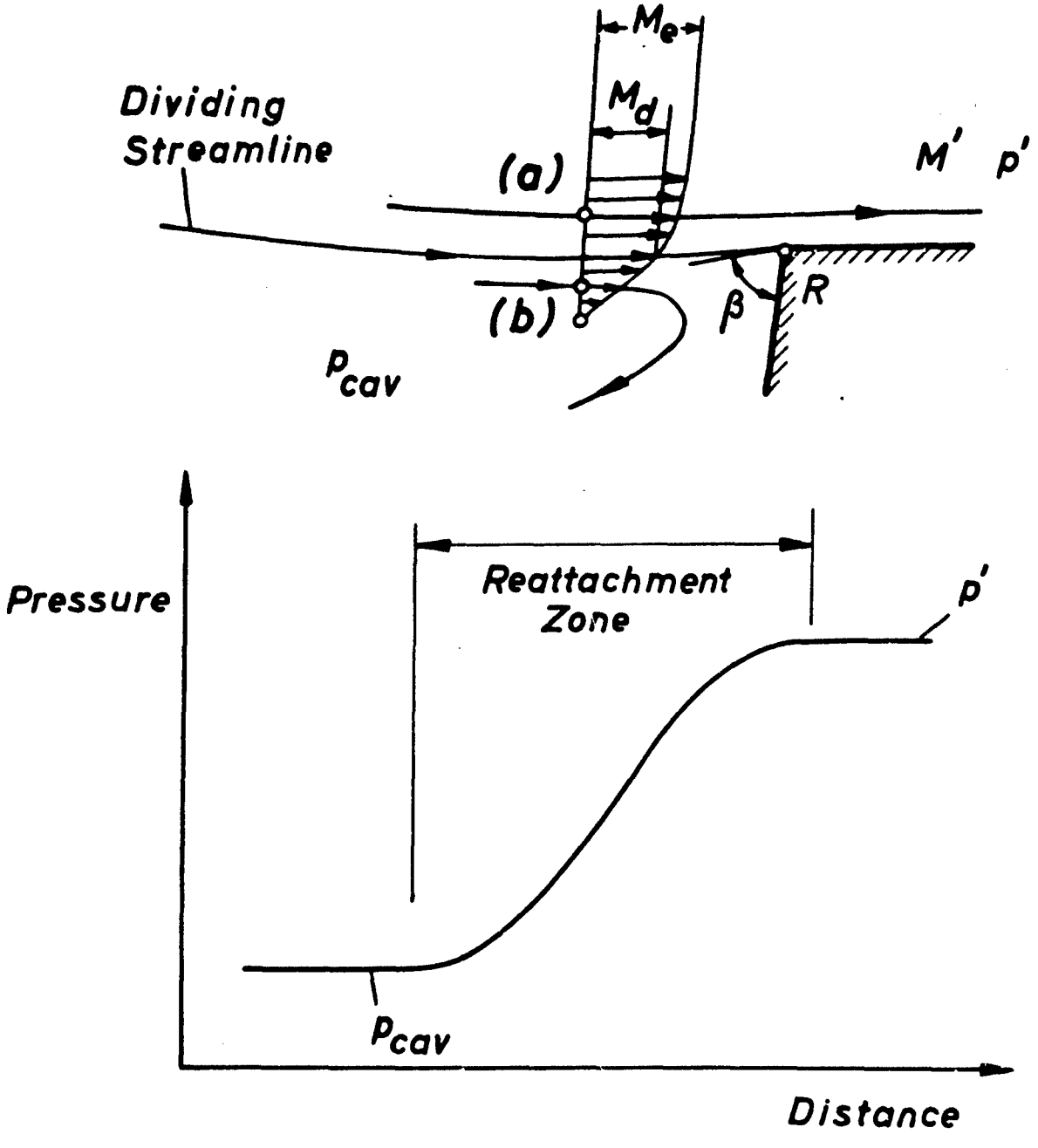

Figure 3 Reattachment Zone

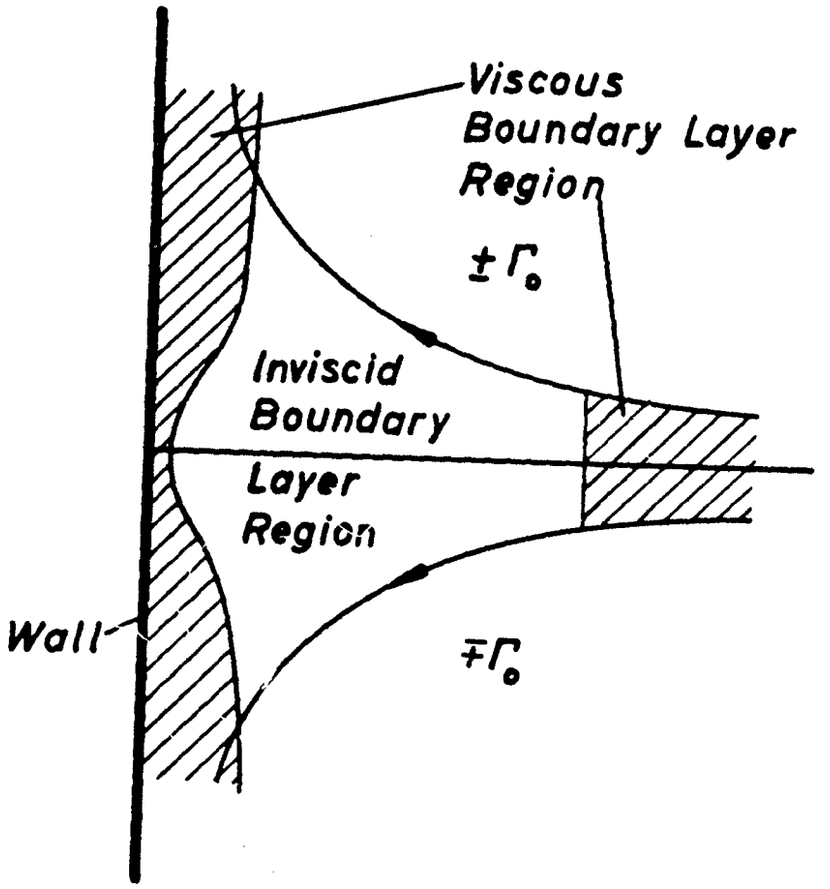

Figure 4 The Flow Near a Stagnation Point on a Rigid Wall (Harper)

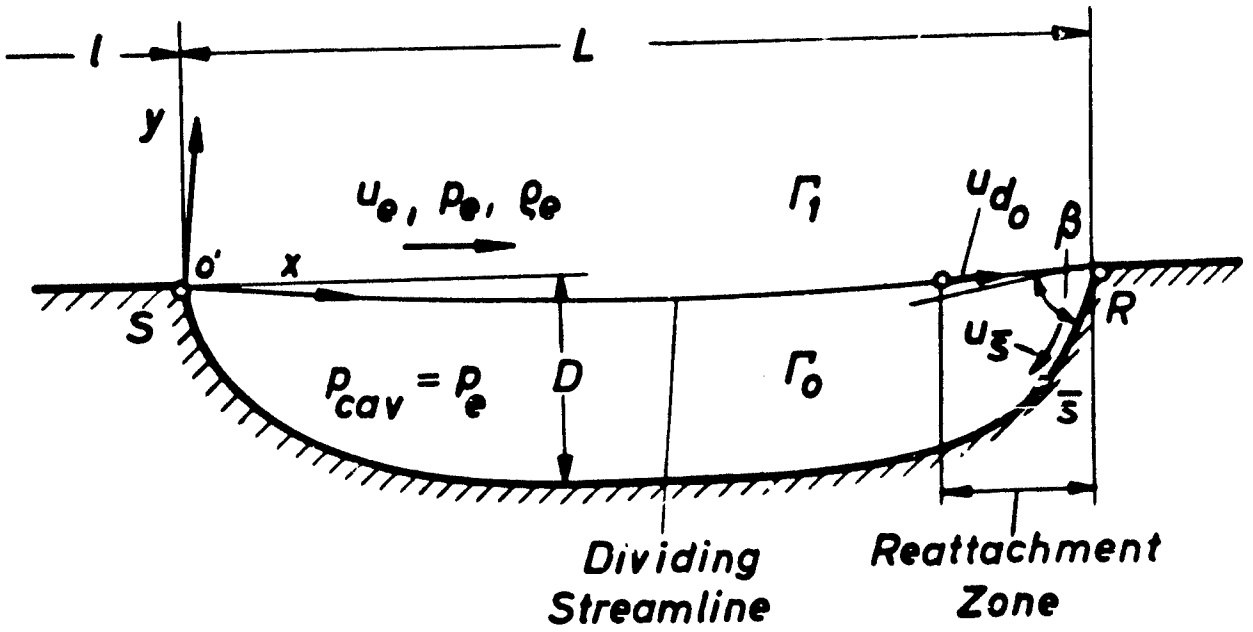

Figure 5 Coordinate System

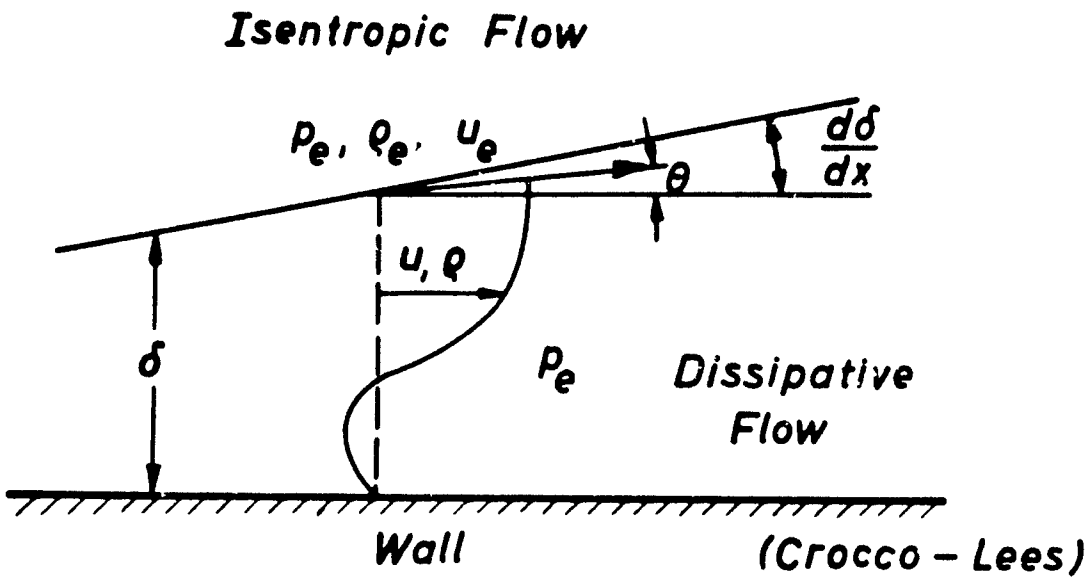

Figure 6 The Two Distinct Flow Regions

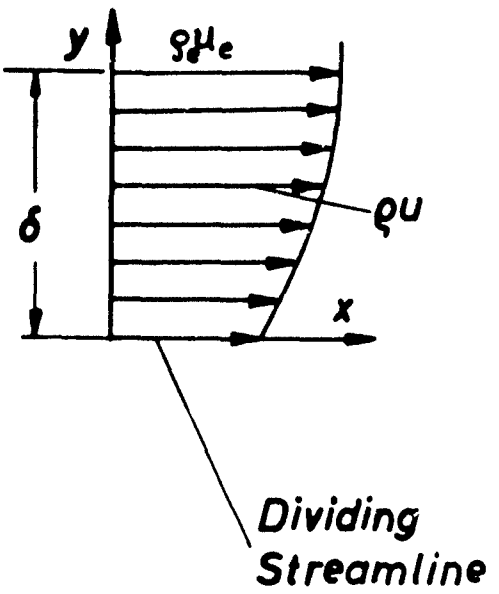

Sketch A

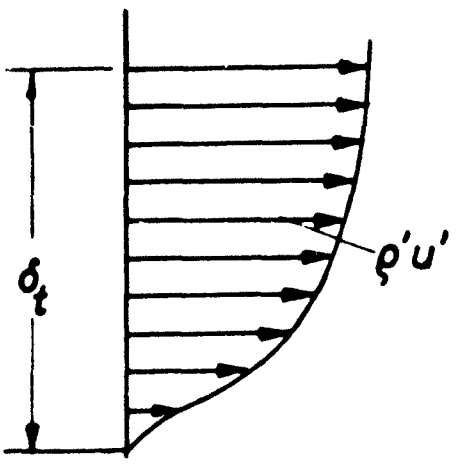

Sketch B

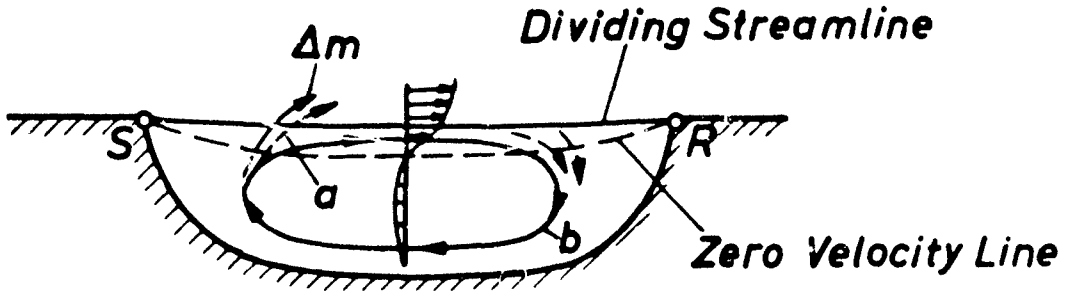

Sketch C

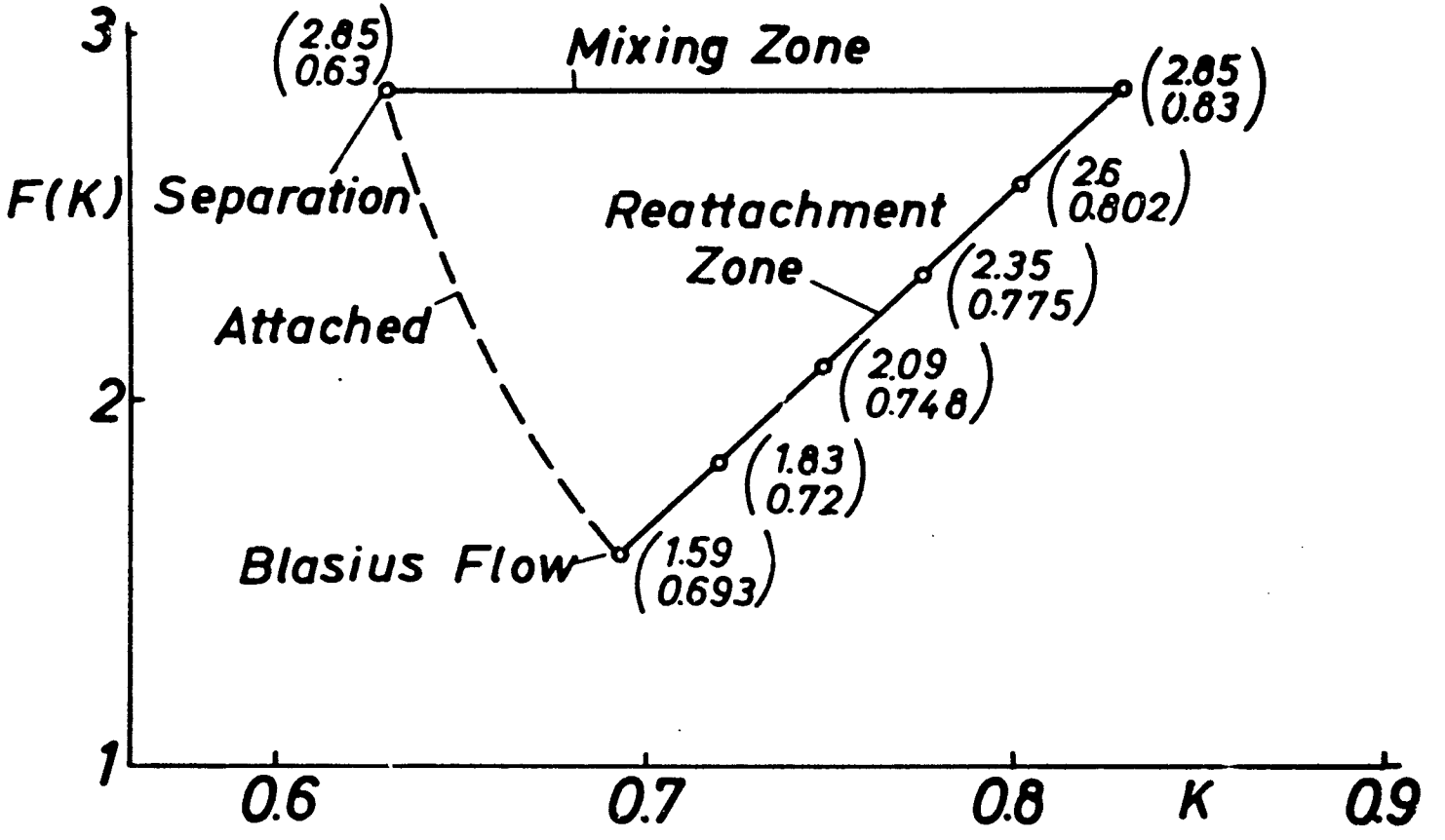

Figure 7 F(K) Trajectory for Laminar Cavity Flow

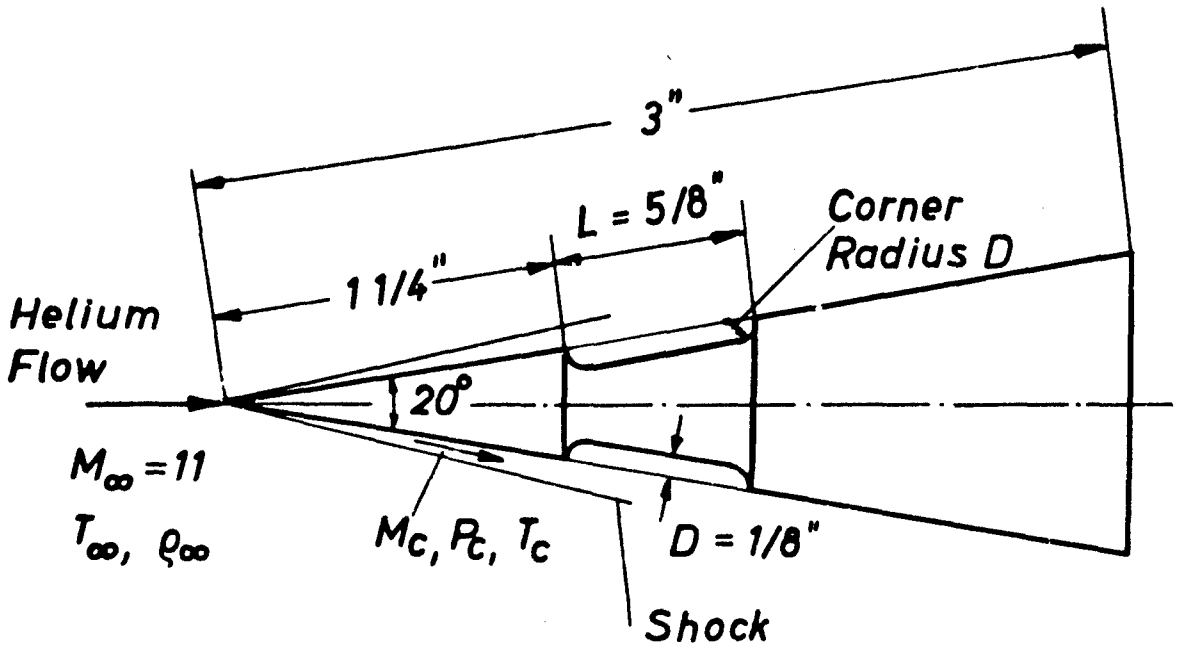

Figure 8 Model Tested

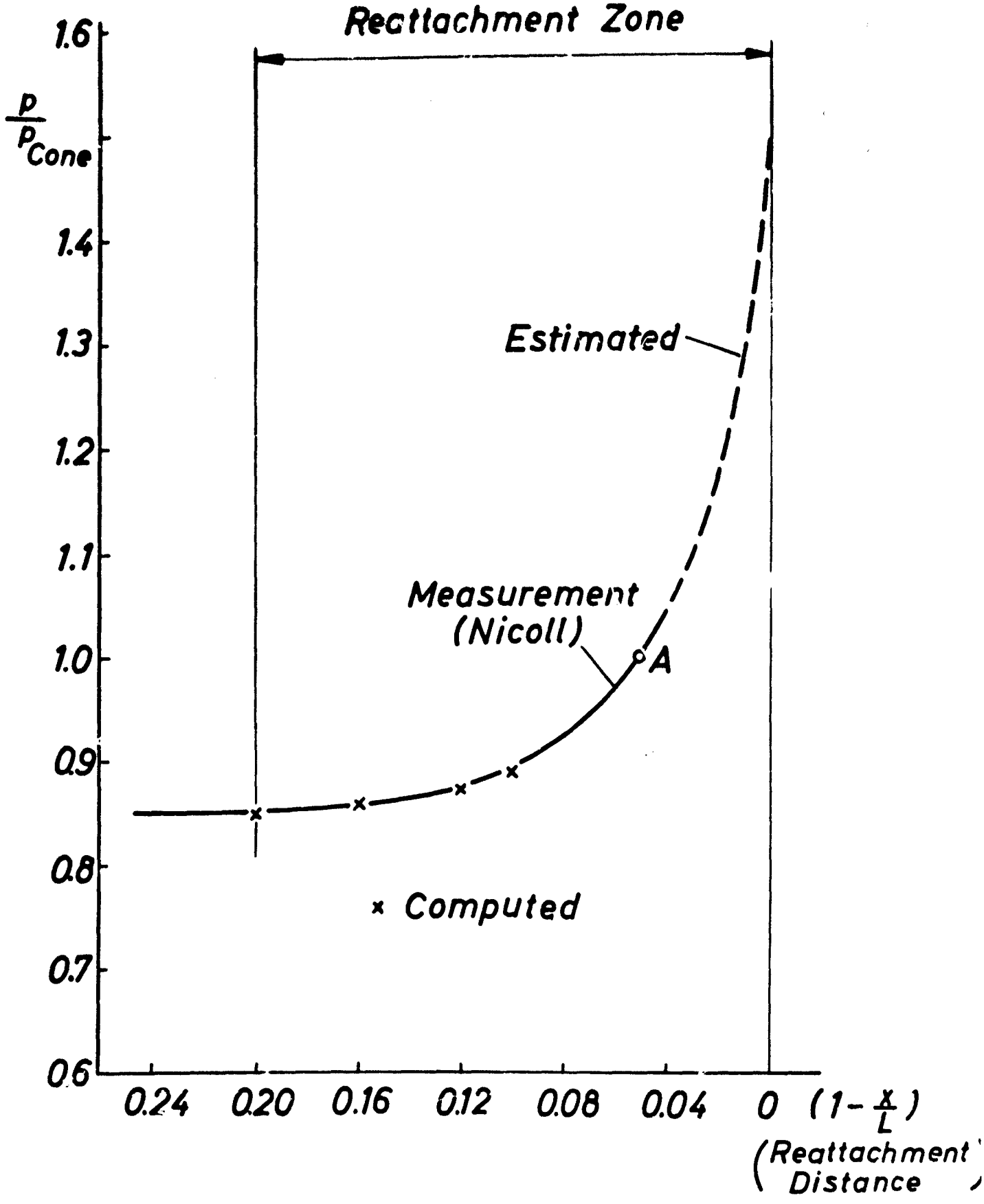

Figure 9 Pressure Rise in Reattachment Zone of Cavity Flow

$P_{St} = 400$ psi a, $M_\infty = 11$, $L/D = 5$

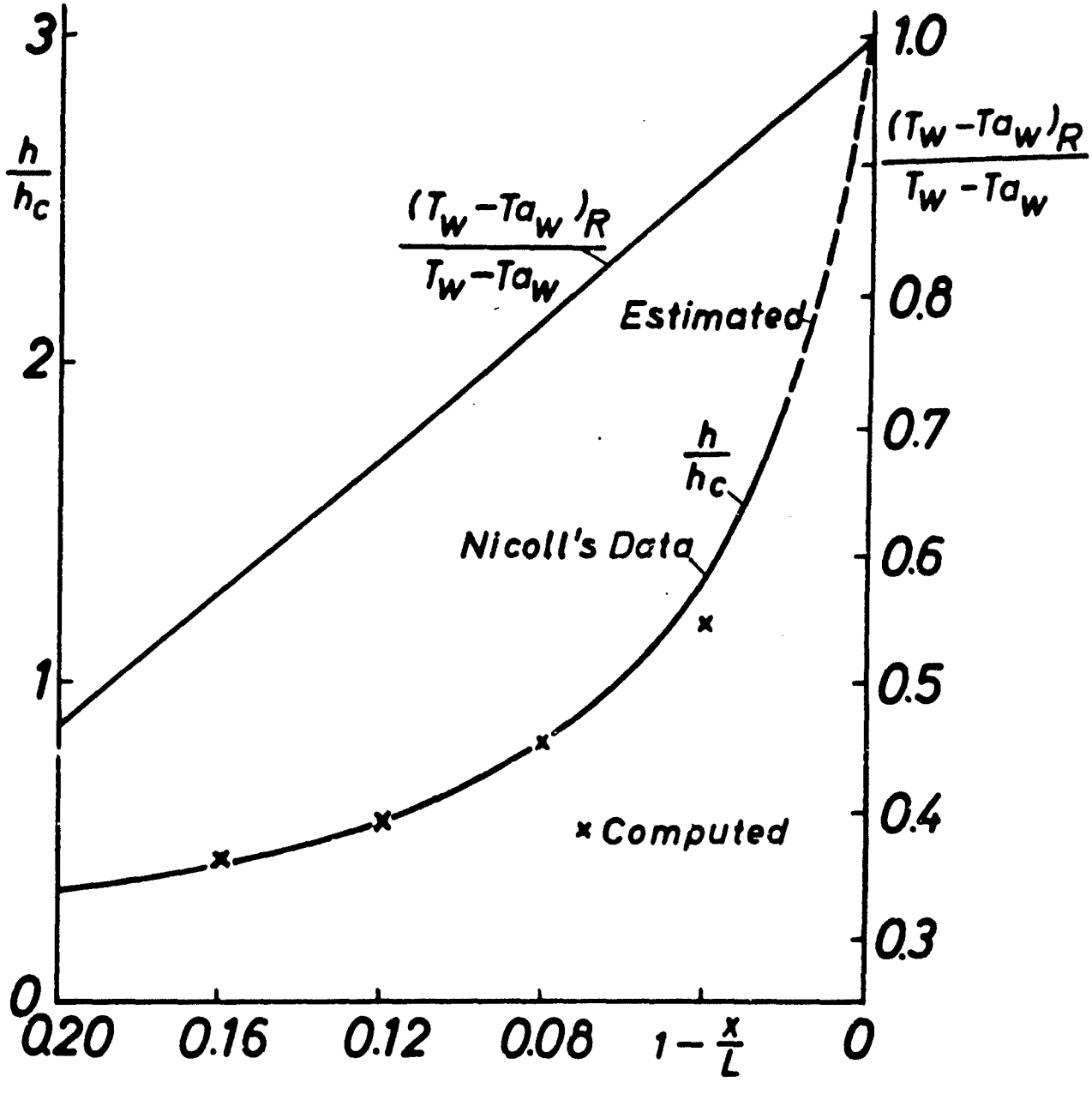

Figure 10 Heat Transfer in Reattachment Zone of Cavity $L = \frac{5}{8}''$ $D = \frac{1}{8}''$

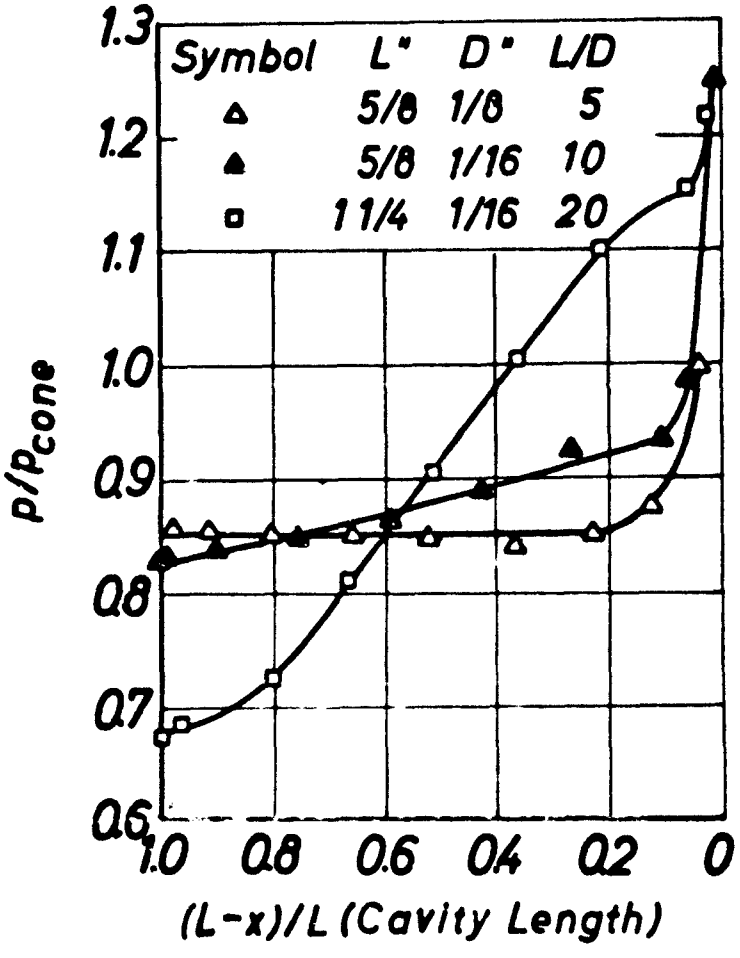

Fig. 11 Cavity Pressure Distributions, p_t = 400 psia (Nicoll)

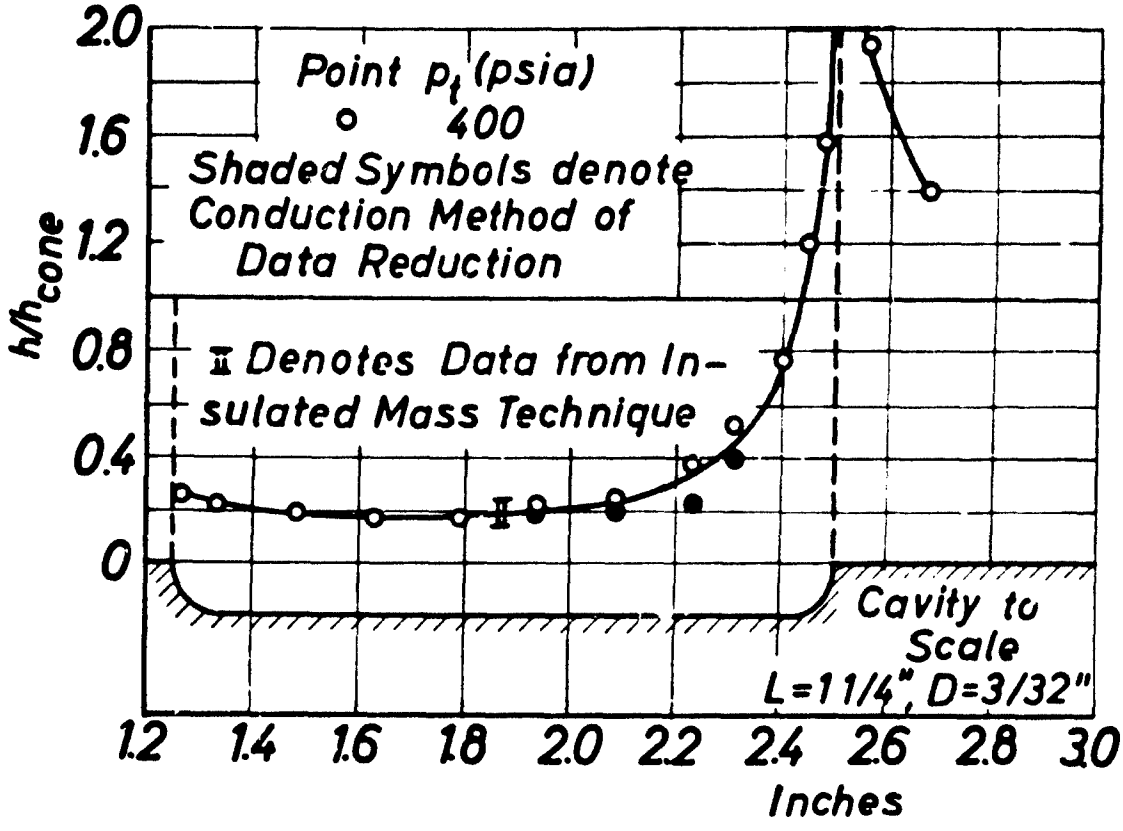

Fig. 12 Local Heat Transfer Coefficient, $L = 1\frac{1}{4}$ In., $D = \frac{3}{32}$ In. (Nicoll)

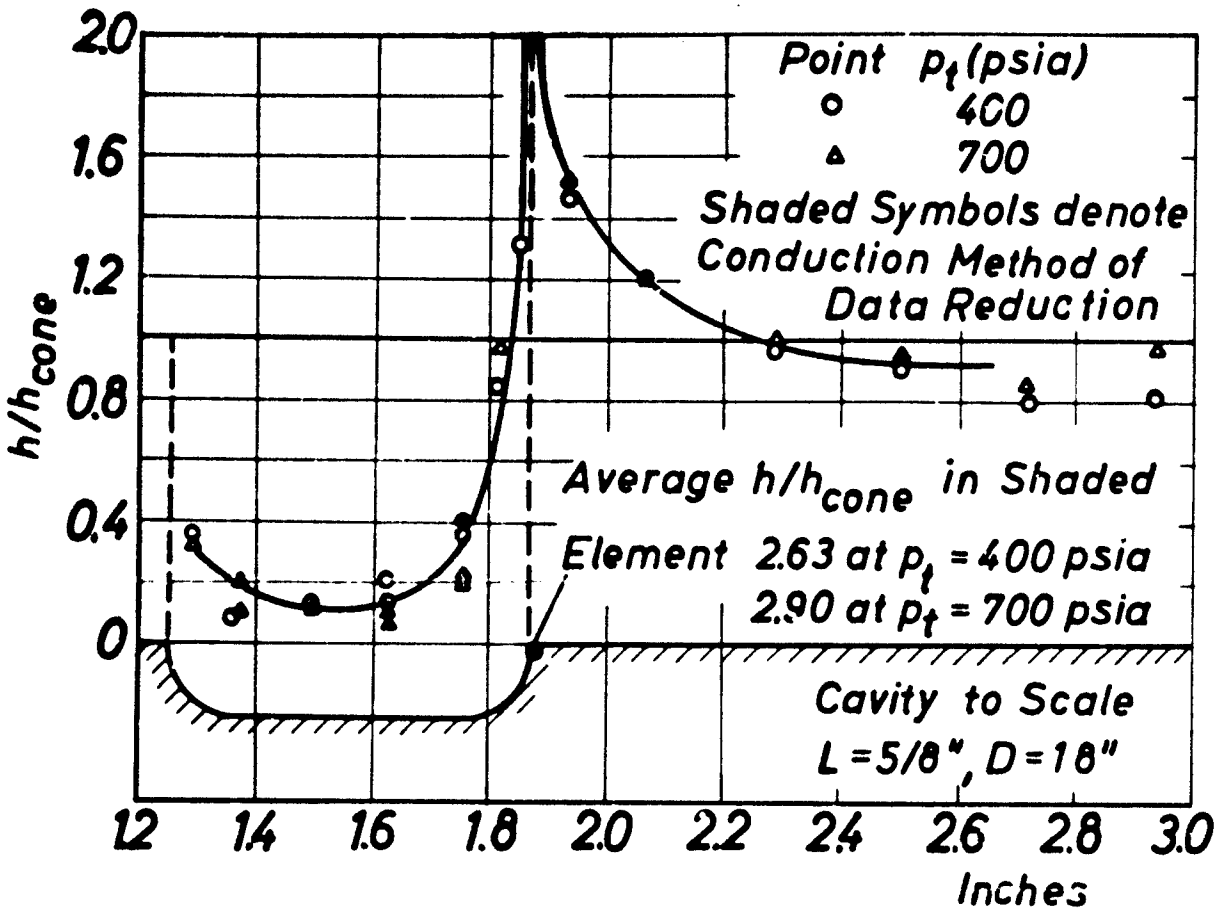

Fig. 13 Local Heat Transfer Coefficient, $L = \frac{5}{8}$ In., $D = \frac{1}{8}$ In. (Nicoll)